A quantum-mechanical perspective on linear response theory within polarizable embedding

Nanna Holmgaard List, Patrick Norman, Jacob Kongsted, and Hans Jørgen Aagaard Jensen

Citation: The Journal of Chemical Physics **146**, 234101 (2017); doi: 10.1063/1.4985565
View online: http://dx.doi.org/10.1063/1.4985565
View Table of Contents: http://aip.scitation.org/toc/jcp/146/23
Published by the American Institute of Physics

A quantum-mechanical perspective on linear response theory within polarizable embedding

Nanna Holmgaard List,[1,a)] Patrick Norman,[1,b)] Jacob Kongsted,[2,c)] and Hans Jørgen Aagaard Jensen[2,d)]
[1]*Division of Theoretical Chemistry and Biology, School of Biotechnology, KTH Royal Institute of Technology, Roslagstullsbacken 15, SE-106 91 Stockholm, Sweden*
[2]*Department of Physics, Chemistry and Pharmacy, University of Southern Denmark, Campusvej 55, 5230 Odense M, Denmark*

(Received 28 February 2017; accepted 30 May 2017; published online 16 June 2017)

We present a derivation of linear response theory within polarizable embedding starting from a rigorous quantum-mechanical treatment of a composite system. To this aim, two different subsystem decompositions (symmetric and nonsymmetric) of the linear response function are introduced and the pole structures as well as residues of the individual terms are discussed. In addition to providing a thorough justification for the descriptions used in polarizable embedding models, this theoretical analysis clarifies which form of the response function to use and highlights complications in separating out subsystem contributions to molecular properties. The basic features of the presented expressions and various approximate forms are illustrated by their application to a composite model system. *Published by AIP Publishing.* [http://dx.doi.org/10.1063/1.4985565]

I. INTRODUCTION

Environments can have profound effects on molecular response and transition properties of a chromophore, yet their modeling comprises a difficult task for quantum-chemical methods. Due to their unfavorable scaling with the system size, a full quantum-mechanical treatment of large molecular systems is out of question when using conventional algorithms. Instead, subsystem approaches in which the system under study is divided into chemically well-defined constituents that are treated individually may be used.

Several methods belong to this category, and one may generally distinguish two different approaches: (*i*) strict subsystem methods that treat the subsystems consistently on an equal footing[1,2] and (*ii*) the so-called embedding approaches in which one particular subsystem is considered to be embedded in the remaining subsystems (the environment). A recent review of subsystem and embedding approaches can be found in Ref. 3. In addition to the obvious computational cost argument, embedding approaches are motivated by the fact that the chemical identity of subsystems is largely intact in molecular complexes and—when targeting excited states—that many electronic transitions are localized in nature. Frozen-density embedding[4] (FDE) provides a formally exact framework through a constrained minimization of the total energy with respect to the density of the embedded subsystem, given that particular conditions on the frozen environment density are fulfilled. For practically achievable frozen densities, it yields an upper bound to the ground-state energy but, if applied in a fully self-consistent manner through freeze-and-thaw cycles,[5] it becomes equivalent to the subsystem reformulation of density functional theory (DFT),[6] thereby bridging (*i*) and (*ii*).[2,7] More efficient, though more approximate embedding approaches are quantum-classical models, such as hybrid quantum mechanics/molecular mechanics methods, involving a discrete but classical representation of the environment.[8–10] These approaches are classified in a hierarchy according to the extent of the coupling between the quantum and classical subsystems,[3] where polarizable embedding (PE) schemes provide the most realistic description accounting for the effects of mutual polarization.[11]

Both subsystem DFT related methods[12–16] and polarizable embedding models[17–22] have been generalized to response formalisms to allow for the calculation of response and transition properties of molecules embedded in large environments. The computational cost associated with the explicit coupling of the subsystem excitation manifolds in a fully coupled scheme generally hinders the inclusion of the dynamical response of the entire environment in large complexes[15] but allows in a truncated form to describe the coupling between selected transitions localized in different subsystems as relevant for chromophoric aggregates.[16] Polarizable embedding, on the other hand, offers an efficient inclusion of the dynamic environment response, provided the perturbing field is nonresonant with respect to local excitations in the environment.[23] This restriction has, however, been lifted by introducing phenomenological excited-state lifetime broadenings in the response formalism.[21,24,25]

So far, extensions of polarizable embedding to quantum-mechanical response theory have been derived assuming a classical description of the environment from the onset of the theoretical treatment. While this is a convenient strategy, the physical origin of the resulting expressions is not

a)Author to whom correspondence should be addressed: nalist@kth.se
b)Electronic mail: panor@kth.se
c)Electronic mail: kongsted@sdu.dk
d)Electronic mail: hjj@sdu.dk

obvious nor what terms are being neglected. The aim of the present work is to formulate a derivation of linear response theory within polarizable embedding starting from a rigorous quantum-mechanical treatment of the entire system. Although various polarizable embedding schemes differ in the specific representation of the environment,[11] their underlying mathematical structure is the same.[26] In this work, we focus on the explicit expressions for the polarizable embedding (PE) model[17,27,28] in which the environment is described in terms of a distributed multipole representation, thus providing a well-defined link to the environment charge density. We note that the main conclusions will also be valid for polarizable density embedding,[29] which go beyond pure polarizable embedding. Our derivation is based on an explicit parameterization of the wave function of the combined system. The origin and inherent limitations become particularly transparent in this framework, where approximations are introduced by imposing restrictions directly on the wave function parameterization.

Whereas previous theoretical analyses have primarily focused on excitation energies,[3,30,31] we shall here be concerned with the general linear response function and not only its poles. Based on the linear response function of the combined system, we derive two different subsystem decompositions, referred to as symmetric and nonsymmetric. These provide a direct connection to the standard response formulations of polarizable embedding based on the classical description of the energy contribution of the interaction with the environment.[28,32] The present theoretical analysis also sheds light on the basic behavior of coupled systems and complications in separating out subsystem contributions to response and transition properties. Finally, key features of the equations are illustrated numerically by considering the linear response of a chromophore–water model complex subject to a weak external electric field.

II. THEORY

In Sec. II A, the basics of the exploited quantum-mechanical direct-product ansatz for the wave function of the combined system will be reviewed; in Sec. II B, this theoretical framework will be used to formulate linear response theory for a composite system; then in Secs. II B 2 and II B 3 we will introduce and compare two different subsystem decompositions to allow for solving the response equations in effective subsystem spaces, creating a connection to basic quantities appearing in the PE model; and in Sec. II B 4, the discussion is extended to a complex response framework, demonstrating how intensity borrowing occurs in a coupled system. Based on the presented subsystem formulations, we will in Sec. II C clarify the connections between a fully quantum-mechanical linear response theory for a selected subsystem in the environment of all other subsystems and when the PE model is used for the environment.

Atomic units (a.u.) will be used throughout.

A. Wave function ansatz: Definitions

Let us consider a composite system consisting of N interacting subsystems, each with an integer number of electrons and with a fixed relative position. In many quantum-classical embedding models, including the PE model which is the main focus in this work, a fundamental assumption is that of nonoverlapping subsystem charge densities [zero-overlap approximation (ZOA)], which implies a strict localization of the subsystem wave functions. The ZOA implies that exchange repulsion vanishes, and as a consequence, the *exact* wave function of the combined system can be written in a basis of direct-product states constructed from the complete antisymmetrized subsystem spaces.[31,33,34] The electronic Hamiltonian for N interacting subsystems decomposes naturally as

$$\hat{\mathcal{H}} = \sum_{A=1}^{N} \hat{\mathcal{H}}_A + \sum_{A>B}^{N} \hat{\mathcal{V}}_{AB}, \tag{1}$$

where $\hat{\mathcal{H}}_A$ is the electronic Hamiltonian of the isolated subsystem A and $\hat{\mathcal{V}}_{AB}$ describes the electrostatic interactions between the nuclei and electrons in the subsystem A with those in B. In second quantization, the interaction operator takes the form

$$\hat{\mathcal{V}}_{AB} = \sum_{m\in B}^{M_B} Z_m \sum_{pq\in A} v_{pq}(\mathbf{R}_m)\hat{E}_{pq} + \sum_{n\in A}^{M_A} Z_n \sum_{rs\in B} v_{rs}(\mathbf{R}_n)\hat{E}_{rs} + \sum_{pq\in A}\sum_{rs\in B} v_{pq,rs}\hat{E}_{pq}\hat{E}_{rs} + \sum_{n\in A}^{M_A}\sum_{m\in B}^{M_B} \frac{Z_n Z_m}{|\mathbf{R}_n - \mathbf{R}_m|}, \tag{2}$$

where v_{pq} and $v_{pq,rs}$ are electrostatic potential and two-electron repulsion integrals, respectively, noting that the two-electron excitation operator within the ZOA factorizes into subsystem contributions, i.e., $\hat{e}_{pq,rs} = \hat{E}_{pq}\hat{E}_{rs}$. The remaining entities have their usual definitions.[35] Occasionally, we will use an alternative representation of the interaction operator,

$$\hat{\mathcal{V}}_{AB} = \int \hat{\rho}_A(\mathbf{r})\hat{\mathcal{V}}_B(\mathbf{r})\mathrm{d}\mathbf{r} = \int \hat{\rho}_B(\mathbf{r})\hat{\mathcal{V}}_A(\mathbf{r})\mathrm{d}\mathbf{r} = \hat{\rho}^A_{\mathbf{r}}\,\hat{\mathcal{V}}^B_{\mathbf{r}}\,, \tag{3}$$

given in terms of the first-order reduced density and electrostatic potential operators as

$$\hat{\rho}_A(\mathbf{r}) = \sum_{n\in A}^{M_A} Z_n \delta(\mathbf{r} - \mathbf{R}_n) - \sum_{pq\in A} \phi^*_p(\mathbf{r})\phi_q(\mathbf{r})\hat{E}_{pq}, \tag{4}$$

$$\hat{\mathcal{V}}_B(\mathbf{r}) = \sum_{m\in B}^{M_B} \frac{Z_m}{|\mathbf{r} - \mathbf{R}_m|} + \sum_{rs\in B} v_{rs}(\mathbf{r})\hat{E}_{rs}. \tag{5}$$

The last equality of Eq. (3) introduces a shorthand notation for the spatial integration with respect to repeated space variables, which will be used in Secs. II B and II C.

As the next step towards effective environment models, the electronic wave function of the combined system is approximated with a single direct product of subsystem wave functions,[33,36]

$$|\Psi_A\Psi_B\ldots\Psi_N\rangle = |\Psi_A\rangle \otimes |\Psi_B\rangle \otimes \cdots |\Psi_N\rangle, \tag{6}$$

which upon variation leads to a set of nonlinear coupled effective subsystem equations to be solved iteratively,

$$\forall\, A: \quad \hat{\mathcal{F}}_A|0_A\rangle = E_A|0_A\rangle. \tag{7}$$

The effective subsystem Hamiltonian reads as

$$\begin{aligned}\hat{\mathcal{F}}_A &= \hat{\mathcal{H}}_A + \sum_{B\neq A}^{N} \langle 0_B|\, \hat{\mathcal{V}}_{AB}\, |0_B\rangle \\ &= \hat{\mathcal{H}}_A + \sum_{pq\in A} \sum_{B\neq A}^{N} \left[\sum_{m\in B}^{M_B} Z_m v_{pq}(\mathbf{R}_m) + \sum_{rs\in B} v_{pq,rs} D_{B,rs} \right] \hat{E}_{pq},\end{aligned} \tag{8}$$

where $D_{B,rs} = \langle 0_B|\, \hat{E}_{rs}\, |0_B\rangle$ is an element of the first-order reduced density matrix for subsystem B. The two terms collected in the square brackets represent the classical electrostatic potential generated by the ground states of the remaining subsystems in their polarized states, i.e., in the presence of the other subsystems.

B. Response theory of composite systems

We will now consider the pure electronic response (i.e., nuclear motions are not included) of the composite system to an external optical field within the framework introduced in Sec. II A. Special attention will be paid to the physical aspects of the intersubsystem interactions in the presence of the applied field and how they influence molecular properties. For notational simplicity, we shall restrict this analysis to two subsystems (leading to an embedded subsystem A and an environment B in polarizable embedding) and work within a configuration interaction (CI) framework for the individual subsystems.

Our derivation for two interacting subsystems is based on the quasi-energy formulation of response theory,[37,38] in which response functions are defined as the coefficients of the time-averaged quasi-energy $\{Q_{AB}\}_T$ in a Taylor series expansion in terms of the external field strengths. Within the ZOA, the field–matter interaction operator describing the action of a monochromatic external field on the composite system can be expressed as

$$\hat{V}^t = \sum_{\pm\omega} \hat{V}^{\omega}_{\alpha} F^{\omega}_{\alpha} e^{-i\omega t} = \sum_{\pm\omega} \left(\hat{V}^{\omega}_{A,\alpha} + \hat{V}^{\omega}_{B,\alpha} \right) F^{\omega}_{\alpha} e^{-i\omega t}, \tag{9}$$

where F^{ω}_{α} are the associated Fourier amplitudes (perturbation strengths). The Greek subscripts indicate (possibly composite) Cartesian labels; and here and henceforth, the Einstein summation convention is adopted for repeated Greek indices.

1. The direct-product approximation

The phase-isolated part of the time-dependent direct-product wave function for the composite system may be defined by an exponential unitary parameterization as

$$\begin{aligned}\widetilde{|0_A 0_B\rangle} &= e^{i\left[\hat{\Lambda}_A(t)+\hat{\Lambda}_B(t)\right]}\, |0_A 0_B\rangle \\ &= e^{i\hat{\Lambda}_A(t)}\, |0_A\rangle \otimes e^{i\hat{\Lambda}_B(t)}\, |0_B\rangle\,; \quad [\hat{\Lambda}_A, \hat{\Lambda}_B] = 0,\end{aligned} \tag{10}$$

where the intersubsystem commutation relation follows from the ZOA. The time-dependent Hermitian operator $\hat{\Lambda}_A(t)$ for subsystem A is parameterized in terms of a set of time-dependent amplitudes $\{\lambda_{i_A}\}$ and takes the form[39]

$$\begin{aligned}\hat{\Lambda}_A(t) &= \sum_{i>0} \left(\lambda_{i_A}(t) \hat{q}^{\dagger}_{i_A} + \lambda^*_{i_A}(t) \hat{q}_{i_A} \right) = \mathbf{Q}^{\dagger}_A \mathbf{\Lambda}_A, \\ \mathbf{Q}^{\dagger}_A &= [\mathbf{q}^{\dagger}_A\ \mathbf{q}_A]; \quad \mathbf{\Lambda}_A = [\boldsymbol{\lambda}_A(t)\ \boldsymbol{\lambda}^*_A(t)]^T,\end{aligned} \tag{11}$$

where an identity operator for subsystem B is implied. The state-transfer operators $\hat{q}^{\dagger}_{i_A} = |i_A\rangle\langle 0_A|$ and their adjoints are built from a set of orthonormalized states $\{|i_A\rangle\}$ that span the orthogonal complement space of the reference state $|0_A\rangle$, the latter satisfying the variational condition given by Eq. (7).

Before proceeding, we briefly comment on the employed parameterization: (*i*) The direct-product parameterization in Eq. (10) is nonlinear, that is, it produces states outside the excitation manifold, defined by the linear action of the operator $\hat{\Lambda}_A(t) + \hat{\Lambda}_B(t)$. In particular, the exponential parameterization contains states in which both subsystems are excited simultaneously due to products of subsystem excitations, despite the absence of such transitions in the state-transfer operators. This is analogous to the nonlinear exponential parameterization of a Hartree–Fock or Kohn–Sham determinant that is based on a generator of single-electron excitations but yet encompasses multi-electron excited determinants. A direct consequence of the use of a nonlinear parameterization is that the properties derived from a response framework differ from those based on the state-specific formulation.[30,31,40–42] (*ii*) The lack of a $\hat{\Lambda}_{AB}(t)$ operator in the exponent of the first equality in Eq. (10) and thus a direct coupling between direct-product states of the types $\langle i_A 0_B|$ and $|i_A j_B\rangle$ as well as $\langle i_A 0_B|$ and $|k_A j_B\rangle$ is the origin of the neglect of state-specific relaxation and London dispersion between the subsystems.[31] (*iii*) The expansion of the time-dependent wave function in the basis of subsystem states means that only intrasubsystem transitions are included, while intersubsystem transitions are excluded. The main assumption imposed by the above parameterization and the conservation of electrons in each subsystem is the exclusion of charge-transfer transitions between the subsystems.

Having settled on an appropriate parameterization of the phase-isolated wave function, explicit expressions for response functions of the combined system can be obtained as perturbation-strength derivatives of the associated time-averaged quasi-energy, evaluated at zero field strengths. The linear response function becomes

$$\langle\langle \hat{V}^{-\omega}_{\alpha}; \hat{V}^{\omega}_{\beta} \rangle\rangle = \left. \frac{\mathrm{d}^2 \{Q_{AB}\}_T}{\mathrm{d}F^{-\omega}_{\alpha}\, \mathrm{d}F^{\omega}_{\beta}} \right|_{\mathbf{F}=\mathbf{0}} = -\mathbf{V}^{\omega\dagger}_{\alpha} (\mathbf{E}^{[2]} - \omega \mathbf{S}^{[2]})^{-1} \mathbf{V}^{\omega}_{\beta}. \tag{12}$$

Ordering the Fourier components of the configuration amplitudes in the operators in Eq. (10) according to $\mathbf{\Lambda}^{\omega} = (\boldsymbol{\lambda}^{\omega}_A, \boldsymbol{\lambda}^{\omega *}_A, \boldsymbol{\lambda}^{\omega}_B, \boldsymbol{\lambda}^{\omega *}_B)^T$ leads to the following intra- and intersubsystem blocked forms of the vectors and matrices:

$$-i\mathbf{V}^{\omega}_{\beta} = \left. \frac{\partial^2 \{Q_{AB}\}_T}{\partial F^{\omega}_{\beta}\, \partial \boldsymbol{\lambda}^{\omega *}} \right|_{\mathbf{F}=\mathbf{0}} = -i \begin{bmatrix} \mathbf{V}^{\omega}_{A,\beta} \\ \mathbf{V}^{\omega}_{B,\beta} \end{bmatrix}, \tag{13}$$

$$\mathbf{E}^{[2]} - \omega \mathbf{S}^{[2]} = \left. \frac{\partial^2 \{Q_{AB}\}_T}{\partial \boldsymbol{\lambda}^{\omega *}\, \partial \boldsymbol{\lambda}^{\omega}} \right|_{\mathbf{F}=\mathbf{0}} = \begin{bmatrix} \mathbf{E}^{[2]}_A & \mathbf{E}^{[2]}_{AB} \\ \mathbf{E}^{[2]}_{BA} & \mathbf{E}^{[2]}_B \end{bmatrix} - \omega \begin{bmatrix} \mathbf{S}^{[2]}_A & \mathbf{0} \\ \mathbf{0} & \mathbf{S}^{[2]}_B \end{bmatrix}. \tag{14}$$

The diagonal blocks of the electronic Hessian and overlap matrices, arising upon differentiation of the quasi-energy with respect to the wave function parameters belonging to the same

subsystem ($I = A, B$), take the same overall form as for the isolated subsystems,

$$\mathbf{E}_I^{[2]} = \begin{bmatrix} \mathbf{A}^I & \mathbf{B}^I \\ \mathbf{B}^{I*} & \mathbf{A}^{I*} \end{bmatrix}, \qquad \mathbf{S}_I^{[2]} = \begin{bmatrix} \mathbf{1} & \mathbf{0} \\ \mathbf{0} & -\mathbf{1} \end{bmatrix}, \qquad \mathbf{V}_{I,\alpha}^{\omega} = \begin{bmatrix} \mathbf{g}_\alpha^I \\ -\mathbf{g}_\alpha^{I\,*} \end{bmatrix}, \tag{15}$$

where the symbols **0** and **1** are used to denote appropriately sized null and identity matrices, respectively. As exemplified for subsystem A, the elements of the subsystem blocks take the form

$$\begin{aligned} A_{ij}^A &= \langle 0_A 0_B | \left[\hat{q}_{i_A}, \left[\hat{\mathcal{H}}_A + \hat{\mathcal{V}}_{AB}, \hat{q}_{j_A}^\dagger \right] \right] | 0_A 0_B \rangle \\ &\overset{\text{CI}}{=} \langle i_A | \hat{\mathcal{H}}_A + \langle 0_B | \hat{\mathcal{V}}_{AB} | 0_B \rangle | j_A \rangle \\ &\quad - \delta_{i_A j_A} \langle 0_A | \hat{\mathcal{H}}_A + \langle 0_B | \hat{\mathcal{V}}_{AB} | 0_B \rangle | 0_A \rangle , \end{aligned} \tag{16}$$

$$\begin{aligned} B_{ij}^A &= \langle 0_A 0_B | \left[\hat{q}_{i_A}, \left[\hat{\mathcal{H}}_A + \hat{\mathcal{V}}_{AB}, \hat{q}_{j_A} \right] \right] | 0_A 0_B \rangle \overset{\text{CI}}{=} 0 , \\ g_{\alpha,i}^A &= \langle 0_A 0_B | [\hat{q}_{i_A}, \hat{V}_{A,\alpha}^{\omega}] | 0_A 0_B \rangle = \langle 0_A | [\hat{q}_{i_A}, \hat{V}_{A,\alpha}^{\omega}] | 0_A \rangle \\ &\overset{\text{CI}}{=} \langle i_A | \hat{V}_{A,\alpha}^{\omega} | 0_A \rangle . \end{aligned} \tag{17}$$

In addition to the isolated subsystem term, the electronic subsystem Hessian in Eq. (15) incorporates a contribution from the intersubsystem coupling. In particular, it describes the coupling between intrasubsystem excitations under the influence of the electrostatic potential produced by the electronic ground state of the other subsystem. The generally rectangular off-diagonal block $\mathbf{E}_{AB}^{[2]}$ and its conjugate transpose $\mathbf{E}_{BA}^{[2]}$ in Eq. (14) describe the intersubsystem coupling. Using the same ordering as in Eq. (15), the structure of this block can be written as

$$\mathbf{E}_{AB}^{[2]} = \begin{bmatrix} \mathbf{\Gamma} & \mathbf{\Theta} \\ \mathbf{\Theta}^* & \mathbf{\Gamma}^* \end{bmatrix}, \tag{18}$$

with elements given by

$$\Gamma_{ij} = \langle 0_A 0_B | \left[\hat{q}_{i_A}, \left[\hat{\mathcal{V}}_{AB}, \hat{q}_{j_B}^\dagger \right] \right] | 0_A 0_B \rangle \overset{\text{CI}}{=} \langle i_A 0_B | \hat{\mathcal{V}}_{AB} | 0_A j_B \rangle , \tag{19}$$

$$\Theta_{ij} = \langle 0_A 0_B | \left[\hat{q}_{i_A}, \left[\hat{\mathcal{V}}_{AB}, \hat{q}_{j_B} \right] \right] | 0_A 0_B \rangle \overset{\text{CI}}{=} -\langle i_A j_B | \hat{\mathcal{V}}_{AB} | 0_A 0_B \rangle . \tag{20}$$

The off-diagonal blocks couple excitations in one subsystem with those in the other, and as follows from these expressions, the coupling is described through a Coulombic interaction of transition densities in the two subsystems. The off-diagonal blocks $\mathbf{S}_{AB}^{[2]}$ and $\mathbf{S}_{BA}^{[2]}$ vanish within the ZOA.

As usual, excitation energies for the combined system can be found as eigenvalues of the generalized eigenvalue equation involving the electronic Hessian and the metric in terms of the overlap matrix,[39]

$$\mathbf{E}^{[2]}\mathbf{X} = \mathbf{S}^{[2]}\mathbf{X}\mathbf{\Omega}. \tag{21}$$

We recall the well-known feature of this generalized eigenvalue problem, where the eigenvalues come in pairs $\pm\omega_n$ and the associated eigenvectors are related,[39,43] and we shall use positive and negative indices ($\omega_{-n} = -\omega_n$) to denote paired solutions. Here, $\mathbf{X}$ is the matrix of eigenvectors satisfying the orthonormality relation

$$\mathbf{X}^\dagger \mathbf{S}^{[2]} \mathbf{X} = \boldsymbol{\sigma}, \qquad \sigma_{nm} = \mathrm{sgn}(n)\delta_{nm}, \tag{22}$$

and $\mathbf{\Omega}$ is the diagonal matrix containing the associated eigenvalues $\pm\omega_n$. For later reference, we introduce the partitioned form of the eigenvector matrix according to the blocked structure in Eq. (14),

$$\mathbf{X} = \begin{bmatrix} \mathbf{X}^A & \mathbf{X}^{AB} \\ \mathbf{X}^{BA} & \mathbf{X}^B \end{bmatrix}, \tag{23}$$

where the off-diagonal blocks describe the degree of delocalization of the excitations in the combined system. The transition strength associated with excitation n in the composite system can then be obtained from the residue analysis of the linear response function as

$$T_{\alpha\beta}^{0n} = \lim_{\omega\to\omega_n} (\omega - \omega_n) \langle\langle \hat{V}_\alpha^{-\omega}; \hat{V}_\beta^{\omega} \rangle\rangle = \mathbf{V}_\alpha^{-\omega_n} \mathbf{X}_n \mathbf{X}_n^\dagger \mathbf{V}_\beta^{\omega_n} \tag{24}$$

and used to compute the dimensionless oscillator strength

$$f_{0n} = \frac{2\omega_n}{3} T_{\alpha\alpha}^{0n}. \tag{25}$$

Having outlined the response formalism for the combined system, our aim of Subsections II B 2 and II B 3 is to obtain expressions for subsystem contributions to properties of the combined system by solving effective equations within the subsystem spaces. These expressions will then be used in Sec. II C to establish a rigorous formulation of linear response theory within polarizable embedding.

2. Subsystem decomposition: Electronic response properties

To decompose the linear response function of the combined system into subsystem contributions, we use the inverse of a blocked matrix with nonsingular square diagonal blocks ($\mathbf{U}$ and $\mathbf{Z}$) which may be written as

$$\begin{bmatrix} \mathbf{U} & \mathbf{V} \\ \mathbf{W} & \mathbf{Z} \end{bmatrix}^{-1} = \begin{bmatrix} (\mathbf{U}-\mathbf{V}\mathbf{Z}^{-1}\mathbf{W})^{-1} & -(\mathbf{U}-\mathbf{V}\mathbf{Z}^{-1}\mathbf{W})^{-1}\mathbf{V}\mathbf{Z}^{-1} \\ -(\mathbf{Z}-\mathbf{W}\mathbf{U}^{-1}\mathbf{V})^{-1}\mathbf{W}\mathbf{U}^{-1} & (\mathbf{Z}-\mathbf{W}\mathbf{U}^{-1}\mathbf{V})^{-1} \end{bmatrix}, \tag{26}$$

which corresponds to using the Löwdin partitioning technique.[44–46] Applying this identity to the matrix resolvent in Eq. (12), we obtain the following subsystem decomposition of the linear response function:

$$\begin{aligned} \langle\langle \hat{V}_\alpha^{-\omega}; \hat{V}_\beta^{\omega} \rangle\rangle &= -\left(\mathbf{V}_{A,\alpha}^{\omega\dagger} \widetilde{\mathbf{N}}_{A,\beta}^{\omega} + \mathbf{V}_{B,\alpha}^{\omega\dagger} \widetilde{\mathbf{N}}_{B,\beta}^{\omega} \right) \\ &= -\mathbf{V}_{A,\alpha}^{\omega\dagger} \left(\widetilde{\mathbf{E}}_A^{[2]}(\omega) - \omega \mathbf{S}_A^{[2]} \right)^{-1} \widetilde{\mathbf{V}}_{A,\beta}^{\omega} \\ &\quad - \mathbf{V}_{B,\alpha}^{\omega\dagger} \left(\widetilde{\mathbf{E}}_B^{[2]}(\omega) - \omega \mathbf{S}_B^{[2]} \right)^{-1} \widetilde{\mathbf{V}}_{B,\beta}^{\omega} . \end{aligned} \tag{27}$$

Since the subsystems are treated on the same footing in this representation, Eq. (27) will in the following be referred to as the symmetric subsystem decomposition (SD). In contrast to Eq. (12), the dimensions in the above expression have been reduced to those of the excitation manifolds of the individual subsystems (e.g., $\dim_A \times \dim_A$) instead of that of the full system ($\dim_A + \dim_B) \times (\dim_A + \dim_B$). As indicated by tildes, the response vectors $\widetilde{\mathbf{N}}_I^{\omega}$ in Eq. (27) are modified quantities that satisfy the following effective linear response equations:

$$\left(\widetilde{\mathbf{E}}_I^{[2]}(\omega) - \omega \mathbf{S}_I^{[2]} \right) \widetilde{\mathbf{N}}_{I,\beta}^{\omega} = \widetilde{\mathbf{V}}_{I,\beta}^{\omega}. \tag{28}$$

In addition to the implicit modifications through the polarization of the reference state vectors (changes induced by

interactions within the subsystem through the interaction part of the diagonal blocks, e.g., $\mathbf{E}_A^{[2]}$), the presence of the other subsystem manifests in explicit contributions to the electronic Hessian and property gradients. In Eqs. (27) and (28), this has been written compactly by introducing effective Hessians and property gradients defined, here for subsystem A, as

$$\widetilde{\mathbf{E}}_A^{[2]}(\omega) = \mathbf{E}_A^{[2]} - \mathbf{E}_{AB}^{[2]}\left(\mathbf{E}_B^{[2]} - \omega\mathbf{S}_B^{[2]}\right)^{-1}\mathbf{E}_{BA}^{[2]}\,, \tag{29}$$

$$\widetilde{\mathbf{V}}_{A,\beta}^{\omega} = \mathbf{V}_{A,\beta}^{\omega} - \mathbf{E}_{AB}^{[2]}\left(\mathbf{E}_B^{[2]} - \omega\mathbf{S}_B^{[2]}\right)^{-1}\mathbf{V}_{B,\beta}^{\omega}\,. \tag{30}$$

These two expressions are key to the present work, showing how the properties of subsystem A are affected by the interacting subsystem. As follows, the coupling between subsystems is governed by three mechanisms. The response vector for subsystem A describes changes induced by (*i*) the indirect coupling through the modification of the pure intrasubsystem term $\mathbf{E}_A^{[2]}$ to include the ground-state electrostatic potential of subsystem B and (*ii*) the explicit coupling to excitations in subsystem B through the frequency-dependent (second) term in the electronic Hessian. A similar result was obtained in the work by Neugebauer in which a subsystem partitioning of the eigenvalue problem within a subsystem DFT response approach is discussed:[16] (*iii*) the direct interaction between the applied external field and subsystem B through the modified property gradient.

The physical meaning of the different terms becomes more clear upon recognizing that the second term in Eq. (29) [in a similar manner for Eq. (30)] can be rewritten, as shown in Sec. S1 of the supplementary material, to give the expression

$$\mathbf{E}_{AB}^{[2]}\left(\mathbf{E}_B^{[2]} - \omega\mathbf{S}_B^{[2]}\right)^{-1}\mathbf{E}_{BA}^{[2]} = \mathbf{V}_{\hat{\nu}_\mathbf{r}}^{A}\, C_{\mathbf{r},\mathbf{r}'}^{B}(\omega)\mathbf{V}_{\hat{\nu}_{\mathbf{r}'}}^{A\dagger}, \tag{31}$$

where $C_{\mathbf{r},\mathbf{r}'}^{B}(\omega) = \langle\langle\hat{\rho}_B(\mathbf{r});\hat{\rho}_B(\mathbf{r}')\rangle\rangle_\omega$ is the frequency-dependent generalized linear polarizability of the polarized ground state of subsystem B (i.e., self-consistently polarized by subsystem A), evaluated at the optical frequency ω.[47] Since the property gradients for subsystem A describe the electrostatic potential generated by the transition density, the last term in Eq. (29) thus describes the linear response of subsystem B induced by the electrostatic potential due to the transition density of subsystem A, which in turn produces an electrostatic potential acting on A. In the same way, the last term of the effective property gradient in Eq. (30) can be interpreted as the electrostatic potential acting on subsystem A due to the linear polarization induced in subsystem B by its direct interactions with the external field. In other words, subsystem B acts as a source of field that gives rise to an effective field strength at the location (but devoid) of subsystem A different from the external field, as represented by $\widetilde{\mathbf{V}}_{A,\beta}^{\omega}$ and $\mathbf{V}_{A,\beta}^{\omega}$, respectively. Note that because of the tensorial nature of the environment polarizability, the external field can be screened differently in different directions. As we shall see in Sec. II C 2, the second terms of Eqs. (29) and (30) reduce to the form of the so-called dynamic reaction field and the effective external field (EEF) effects appearing in polarizable embedding.[28,32]

Finally, we note that neither of the subsystem contributions to the linear response function in Eq. (27) is symmetric with respect to the left and right property gradients. For that reason, there is no guarantee that the effective subsystem polarizability tensors are symmetric, as discussed before,[15] or that the diagonal elements are positive in the static limit. This is in contrast to the polarizability tensor of the combined system, which is symmetric, as it should be. Physically, the individual terms in the symmetric decomposition can be viewed as describing the linear response of a property associated with the operator $\hat{V}_{A,\alpha}^{-\omega}$ to the actual perturbing field acting on subsystem A in the presence of subsystem B.

3. Subsystem decomposition: Electronic transition properties

We now continue with an analysis of the transition properties of the composite system. As pointed out in the Introduction, the lowest electronic transitions are often localized in nature and can often be attributed predominantly to a particular subsystem, i.e., the excitation vectors have the dominant contribution in the excitation manifold of one of the subsystems. Rather than solving the full generalized eigenvalue equation in Eq. (21), the excitation energies of the combined system may be determined from the effective response equations in Eq. (28) upon zeroing the right-hand sides. Folding the effects of subsystem B into the equation for A yields the following pseudo-generalized eigenvalue equation:

$$\widetilde{\mathbf{E}}_A^{[2]}(\omega_n)\widetilde{\mathbf{X}}_n^A = \omega_n\mathbf{S}_A^{[2]}\widetilde{\mathbf{X}}_n^A\,, \tag{32}$$

which has the dimension of the excitation manifold of subsystem A. Provided there are no degenerate states located in the B part, the excitation energies derived from the reduced system in Eq. (32) are identical to those associated with the subsystem A part of the parent system in Eq. (21). This reformulation thus turns the generalized eigenvalue problem for the full system into a dressed subsystem problem, as has been shown before in the subsystem DFT response framework.[16] In other words, this form allows us to compute the poles associated with the A block of Eq. (21) without having to consider the full problem with the dimension of both subsystems. This is particularly attractive for determining localized transitions as relevant from the perspective of embedding calculations. The nonlinearity of Eq. (32) introduced by the frequency-dependent effective Hessian, however, requires knowledge of the solutions beforehand or that the problem is solved iteratively one excitation at a time, including the construction of a new Hessian for each eigenvalue in question. As a consequence, the subsystem A components will not be orthogonal to each other (only the full eigenvectors will). For later reference, we introduce the frozen ground-state polarization (FP) approximation in which only the subsystem term $\mathbf{E}_A^{[2]}$ is included in Eq. (32), i.e., subsystem B is not allowed to respond to the density changes in A upon excitation (that is, neglecting intersubsystem couplings).

Let us return to the evaluation of the transition strengths associated with the excitations in the composite system, but now taking a decomposed form of the linear response function as a starting point. As should become more clear from the numerical illustration in Sec. III, each subsystem contribution to the response function [i.e., symmetric decomposition in Eq. (27)] displays poles at all excitations in the combined system. This is not compliant with our heuristic view on

local excitations but is a natural consequence of the delocalization present in coupled systems.[48] However, it implies that transition strengths of electronic transitions "localized" in subsystem A cannot be identified as the residues of the subsystem A contribution to the response function [the first term in Eq. (27)].

To facilitate the identification of residues, we introduce an alternative partitioning of the matrix resolvent in Eq. (12), which can be obtained by applying the Woodbury matrix identity (for nonsingular square matrices $\mathbf{U}$ and $\mathbf{Z}$)

$$(\mathbf{Z}-\mathbf{W}\mathbf{U}^{-1}\mathbf{V})^{-1}\mathbf{W}\mathbf{U}^{-1} = \mathbf{Z}^{-1}\mathbf{W}(\mathbf{U}-\mathbf{V}\mathbf{Z}^{-1}\mathbf{W})^{-1}, \tag{33}$$

$$(\mathbf{Z}-\mathbf{W}\mathbf{U}^{-1}\mathbf{V})^{-1} = \mathbf{Z}^{-1}+\mathbf{Z}^{-1}\mathbf{W}(\mathbf{U}-\mathbf{V}\mathbf{Z}^{-1}\mathbf{W})^{-1}\mathbf{V}\mathbf{Z}^{-1}, \tag{34}$$

to the third and fourth blocks of Eq. (26) (alternatively, the first and second blocks to get the residues related to the B part). Hereby, the linear response function of the combined system can be written as

$$\begin{aligned}\langle\langle \hat{V}_\alpha^{-\omega}; \hat{V}_\beta^{\omega}\rangle\rangle = &-\widetilde{\mathbf{V}}_{A,\alpha}^{\omega\dagger}\left(\widetilde{\mathbf{E}}_A^{[2]}-\omega\mathbf{S}_A^{[2]}\right)^{-1}\widetilde{\mathbf{V}}_{A,\beta}^{\omega}\\ &-\mathbf{V}_{B,\alpha}^{\omega\dagger}\left(\mathbf{E}_B^{[2]}-\omega\mathbf{S}_B^{[2]}\right)^{-1}\mathbf{V}_{B,\beta}^{\omega}\,.\end{aligned} \tag{35}$$

Contrary to Eq. (27), the subsystems are now treated on an unequal footing, and therefore Eq. (35) will be referred to as the nonsymmetric decomposition (NSD). We note that the same approach was used in the original formulations of second-order polarization propagator approximation (SOPPA) theory[49] in which the effective quantities described the doubles correction to the particle-hole spectrum, while the pure double excitations were given by the second term. As will be discussed in Sec. II C 2, the expressions for polarizable embedding in a linear response framework follow, in a similar spirit as SOPPA and algebraic diagrammatic construction,[50] from a perturbation analysis of the individual matrices appearing in Eq. (35).

An important outcome of this alternative representation of the response function of the combined system is that the poles of the A-dominated excitations (all excitations of the composite system) are contained entirely in the first term. However, as a consequence of the second term, the partitioning in Eq. (35) introduces additional poles in the individual terms at the transition frequencies of the ground-state polarized subsystem B. Hence, the correct pole structure for the composite system is only recovered upon taking the sum of the two terms. Nevertheless, the first term in Eq. (35) can be used to identify the correct decomposed expression for the residues of the excitations mainly in subsystem A, since the second term does not affect excitation energies and transition moments but is needed only in the calculation of the response function.

Until now, the normalization of the effective eigenvectors obtained from Eq. (32) has been of no concern since it does not affect excitation energies. However, it is necessary to consider renormalization of the effective eigenvectors upon the evaluation of transition strengths in the decomposed formulation. In particular, since the eigenvector of the full equation, corresponding to a transition mainly localized in subsystem A, is normalized to ± 1 according to

$$\mathbf{X}_n^{A\dagger}\mathbf{S}_A^{[2]}\mathbf{X}_n^{A} + \mathbf{X}_n^{BA\dagger}\mathbf{S}_B^{[2]}\mathbf{X}_n^{BA} = \sigma_n, \tag{36}$$

the norm of the subsystem A component (first term) must be less than unity. The A and B components of the eigenvector are related through Eq. (21), which can be used to rewrite the normalization condition in terms of the A component. This leads to the following renormalization factor for the effective eigenvector for the given pole ω_n:

$$\begin{aligned}(\Gamma_n^A)^{-1} = &\widetilde{\mathbf{X}}_n^{A\dagger}\mathbf{S}_A^{[2]}\widetilde{\mathbf{X}}_n^{A} + \widetilde{\mathbf{X}}_n^{A\dagger}\mathbf{E}_{AB}^{[2]}(\mathbf{E}_B^{[2]}-\omega_n\mathbf{S}_B^{[2]})^{-1}\\ &\times\mathbf{S}_B^{[2]}(\mathbf{E}_B^{[2]}-\omega_n\mathbf{S}_B^{[2]})^{-1}\mathbf{E}_{BA}^{[2]}\widetilde{\mathbf{X}}_n^{A}.\end{aligned} \tag{37}$$

The transition strength between the ground state and an excited state mainly located in subsystem A can then be written, in the decomposed form, as

$$T_{\alpha\beta}^{0n} = \Gamma_n^A\widetilde{\mathbf{V}}_{A,\alpha}^{-\omega_n}\widetilde{\mathbf{X}}_n^{A}\widetilde{\mathbf{X}}_n^{A\dagger}\widetilde{\mathbf{V}}_{A,\beta}^{\omega_n}\,. \tag{38}$$

What we have achieved up to this point is to recast Eqs. (12) and (21) into dressed subsystem expressions that separate out subsystem contributions to molecular and transition properties of the combined system. As will become clear from the final steps taken in Sec. II C, this provides a justification of the various environmental effects appearing in polarizable embedding. Importantly, the theoretical analysis has enlightened what decomposed form of the response function to use for a specific purpose. We remark that such clarification does not follow from a derivation anticipating the classical description of the environment in the first place, where the Ehrenfest and quasi-energy derivative formulations of response theory lead to different response functions [see discussion below Eq. (20) in Ref. 51].

Although the subsystem decompositions given above based on standard response theory are illustrative and provide insight into the mechanisms governing the interaction between subsystems, their practical application for transition properties is limited for several reasons: (*i*) the solution of the pseudo-generalized eigenvalue problem in Eq. (32) requires an iterative scheme, (*ii*) a new effective subsystem A Hessian has to be constructed for each "eigenvalue" of interest, and (*iii*) the problem is ill-defined if poles in subsystem B are too close to the one being solved for. In addition, the normalization factor in Eq. (37) cannot be straightforwardly converted into an effective environment analog, as needed when turning to embedding models, because it cannot be rewritten in terms of the response kernel of the environment. These complications can be avoided by switching to a complex response theory framework in which transition properties can be computed without having to resolve the individual excitations. Another interesting use of this framework as will be explored next is to demonstrate the intensity borrowing that occurs between interacting subsystems.

4. Subsystem decomposition in a complex response framework

In complex response theory, effects of radiative and nonradiative relaxation mechanisms for the decay of the excited states are modeled in a phenomenological manner by assigning finite lifetimes (τ_n) to the excited states. This leads to complex-valued response functions that are well-defined across the

entire frequency range and thus provides resonant-convergent properties. The complex linear response function takes the following form:[52–54]

$$\langle\langle \hat{V}_\alpha^{-\omega}; \hat{V}_\beta^{\omega} \rangle\rangle = -\mathbf{V}_\alpha^{\omega\dagger}(\mathbf{E}^{[2]} - (\omega + i\boldsymbol{\gamma})\mathbf{S}^{[2]})^{-1}\mathbf{V}_\beta^{\omega}\,, \tag{39}$$

where we, as customary, have adopted a common lifetime, and hence damping parameter $\gamma = (2\tau)^{-1}$, for all excited states, simplifying the relaxation matrix to $\boldsymbol{\gamma} = \gamma\mathbf{1}$.

Similar to the conventional response framework, the complex linear response function may be expressed in alternative subsystem decomposed forms. Applying Eq. (26) and rewriting according to Eqs. (33) and (34) yield the nonsymmetric subsystem decomposition

$$\begin{aligned}\langle\langle \hat{V}_\alpha^{-\omega}; \hat{V}_\beta^{\omega} \rangle\rangle = &-\widetilde{\mathbf{V}}_{A,\alpha}^{\omega\dagger'}(\widetilde{\mathbf{E}}_A^{[2]}(\omega) - (\omega + i\gamma)\mathbf{S}_A^{[2]})^{-1}\widetilde{\mathbf{V}}_{A,\beta}^{\omega} \\ &- \mathbf{V}_{B,\alpha}^{\omega\dagger}(\mathbf{E}_B^{[2]} - (\omega + i\gamma)\mathbf{S}_B^{[2]})^{-1}\mathbf{V}_{B,\beta}^{\omega}, \end{aligned}\tag{40}$$

where the effective subsystem vector and matrix quantities are now complex, here given for subsystem A,

$$\widetilde{\mathbf{E}}_A^{[2]}(\omega) = \mathbf{E}_A^{[2]} - \mathbf{E}_{AB}^{[2]}(\mathbf{E}_B^{[2]} - (\omega + i\gamma)\mathbf{S}_B^{[2]})^{-1}\mathbf{E}_{BA}^{[2]}\,, \tag{41}$$

$$\widetilde{\mathbf{V}}_{A,\alpha}^{\omega} = \mathbf{V}_{A,\alpha}^{\omega} - \mathbf{E}_{AB}^{[2]}(\mathbf{E}_B^{[2]} - (\omega + i\gamma)\mathbf{S}_B^{[2]})^{-1}\mathbf{V}_{B,\alpha}^{\omega}. \tag{42}$$

It should be noted that the conjugate transpose of the effective quantities is assumed here, as indicated by the prime, to act only on vectors and matrices but without changing the sign in front of the damping parameter.

Our aim is to show intensity borrowing between the coupled subsystems and how it manifests in the subsystem decomposed formulation. To this end, we shall make use of the fact that the imaginary part of the complex electric dipole–dipole polarizability is proportional to the linear absorption cross section $\sigma(\omega)$[55,56] along with its relation via the integrated absorption cross section to the sum of oscillator strengths (see Sec. S2 of the supplementary material). Assuming an isotropic sample with respect to the light polarization, we have

$$\sigma(\omega) = \frac{\omega}{3\epsilon_0 c_0}\mathrm{Im}\left[\alpha_{\alpha\alpha}(\omega)\right] \tag{43}$$

and

$$I = \int_0^\infty \sigma(\omega)\,\mathrm{d}\omega = \frac{\pi}{2\epsilon_0 c_0}\sum_{n>0} f_{n0}\,, \tag{44}$$

where ϵ_0 is the vacuum permittivity and c_0 is the speed of light in vacuum. In the framework of exact state theory or variational approximate state theory in the complete basis set limit, the Thomas–Reiche–Kuhn sum rule further implies that the sum of oscillator strengths is equal to the number of the electrons in the system N_e. Accordingly, for the combined system, we have

$$\sum_{n>0} f_{n0}^{AB} = N_\mathrm{e}^A + N_\mathrm{e}^B\,, \tag{45}$$

and likewise for the subsystems,

$$\sum_{n>0} f_{n0}^{\mathrm{vac},I} = \sum_{n>0} f_{n0}^{\mathrm{FP},I} = N_\mathrm{e}^I, \qquad I = A, B. \tag{46}$$

Together, Eqs. (44) and (45) reflect that excitations in one subsystem can borrow intensity from transitions in the other subsystem, while the total integrated cross section is preserved. By combining Eqs. (44)–(46) and recalling that the second term of the complex linear response function in the nonsymmetric decomposition [Eq. (40)] is identical to the linear response function of subsystem B within the FP approximation, it follows that

$$\int \sigma_1^{\mathrm{NSD}}(\omega)\,\mathrm{d}\omega = \frac{\pi}{2\epsilon_0 c_0}N_\mathrm{e}^A, \quad \int \sigma_2^{\mathrm{NSD}}(\omega)\,\mathrm{d}\omega = \frac{\pi}{2\epsilon_0 c_0}N_\mathrm{e}^B, \tag{47}$$

where σ_1^{NSD} and σ_2^{NSD} denote the contributions to the absorption cross section from the first and second terms in Eq. (40), respectively.

It thus follows that if an A-dominated transition gains in intensity due to coupling to excitations in subsystem B, then $\sigma_1^{\mathrm{NSD}}(\omega)$ will take on negative values around poles in subsystem B. Consequently, in these regions of the spectrum, $\sigma_1^{\mathrm{NSD}}(\omega)$ in itself cannot be associated with an absorption spectrum but it rather becomes imperative to consider the total absorption cross section $\sigma(\omega)$. This discussion is important due to its implications in the context of polarizable embedding (Sec. II C) in which one focuses on the calculation of $\sigma_1^{\mathrm{NSD}}(\omega)$ and, as we have seen, caution is called for in the interpretation of the results of such a calculation (see Sec. III).

C. Polarizable embedding

Having derived the expressions for the direct-product ansatz for the combined system, our aim in this section is to recover the quantum-mechanical linear response treatment within the PE model. The subsystems will now be treated at different levels, where a classical description will be adopted for subsystem B. To reflect this distinction, subsystem A will in this section be referred to as the quantum region and B as the environment. Furthermore, instead of considering the environment as a whole, the individual subsystems constituting the environment $B = \{b_1, b_2, \ldots, b_{N-1}\}$ will be treated separately by decomposing the environment wave function into a product of subsystem contributions, still assuming nonoverlapping subsystem charge densities. We will assume that the unperturbed (i.e., vacuum) environment subsystem eigenfunctions and eigenenergies $\{|0_b^{(0)}\rangle, |j_b^{(0)}\rangle\}$ and $\{E_{0_b}^{(0)}, E_{j_b}^{(0)}\}$, for $b \in B$, are known, where superscripts (n) specify the order with respect to the perturbation.

1. Working equations

In the PE model, we invoke a perturbation treatment of all but subsystem A and assume that the environment is only linearly responsive. This corresponds to requiring that Eq. (7) for $b \in B$ is fulfilled only through first order in terms of the electrostatic potentials from the ground states of the other subsystems. Within this approximation, the interaction operator acting on subsystem A takes the form

$$\begin{aligned}\hat{\mathcal{V}}^{\mathrm{int}} = &\underbrace{\sum_{pq\in A}\sum_{b\in B}\sum_{m\in b}^{M_b} Z_m\left[v_{pq}(\mathbf{R}_m) + \sum_{rs\in b} v_{pq,rs}D_{b,rs}^{(0)}\right]\hat{E}_{pq}}_{\hat{\mathcal{V}}^{\mathrm{es}}} \\ &+ \underbrace{\sum_{pq\in A}\sum_{b\in B}\sum_{rs\in b} v_{pq,rs}D_{b,rs}^{(1)}\hat{E}_{pq}}_{\hat{\mathcal{V}}^{\mathrm{ind}}}\,, \end{aligned}\tag{48}$$

consisting of contributions from the permanent and induced charge distributions, $\hat{\mathcal{V}}^{\mathrm{es}}$ and $\hat{\mathcal{V}}^{\mathrm{ind}}$, respectively, of the environment subsystems. In terms of the first-order reduced density and electrostatic potential operators in Eqs. (4) and (5), they read

$$\hat{\mathcal{V}}^{\mathrm{es}} = \sum_{b\in B} \int \hat{\rho}^{\mathrm{e}}_A(\mathbf{r}) \langle \hat{\mathcal{V}}_b(\mathbf{r}) \rangle^{(0)}_{0_b} \, \mathrm{d}\mathbf{r} \,, \tag{49}$$

$$\hat{\mathcal{V}}^{\mathrm{ind}} = \sum_{b\in B} \int \hat{\rho}^{\mathrm{e}}_A(\mathbf{r}) \langle \hat{\mathcal{V}}_b(\mathbf{r}) \rangle^{(1)}_{0_b} \, \mathrm{d}\mathbf{r} \,, \tag{50}$$

where superscript "e" signifies that only the electronic part of the operator is included. We have further introduced a shorthand notation for expectation values, e.g., $\langle \hat{\mathcal{V}}_b(\mathbf{r}) \rangle^{(0)}_{0_b} = \left\langle 0^{(0)}_b \middle| \hat{\mathcal{V}}_b(\mathbf{r}) \middle| 0^{(0)}_b \right\rangle$.

As shown in detail in Sec. S3 of the supplementary material, substitution of the first-order correction to the wave function of subsystem b into $\hat{\mathcal{V}}^{\mathrm{ind}}$ and introducing a multipole representation of the electrostatic potential operator, the electrostatic and induction operators can be rewritten in a three-dimensional multi-index notation as

$$\hat{\mathcal{V}}^{\mathrm{es}} = \sum_{pq\in A} \sum_{b\in B} \sum_{|k|=0}^{\infty} \frac{(-1)^{|k|}}{k!} M^{(k)}_b t^{(k)}_{pq}(\mathbf{R}_b) \hat{E}_{pq}, \tag{51}$$

$$\hat{\mathcal{V}}^{\mathrm{ind}} = -\sum_{b\in B} \sum_{|k|=1}^{\infty} \frac{1}{k!} \hat{F}^{\mathrm{e},(k)}_A(\mathbf{R}_b) \bar{M}^{(k)}_b \tag{52}$$

$$= -\sum_{b\in B} \sum_{|k|=1}^{\infty} \sum_{|l|=1}^{\infty} \frac{1}{k!\cdot l!} \hat{F}^{\mathrm{e},(k)}_A(\mathbf{R}_b) P^{(k,l)}_b \times \left(\langle \hat{F}^{(l)}_A(\mathbf{R}_b) \rangle_{0_A} + \sum_{b'\in B\setminus b} \left[\langle \hat{F}^{(l)}_{b'}(\mathbf{R}_b) \rangle^{(0)}_{0_{b'}} + \langle \hat{F}^{(l)}_{b'}(\mathbf{R}_b) \rangle^{(1)}_{0_{b'}} \right] \right), \tag{53}$$

where $t^{(k)}_{pq}$ is the electrostatic potential integral, $P^{(k,l)}_b$ are static electronic polarizabilities of subsystem b, analogous to that in Eq. (31), and $\hat{F}^{(k)}_A(\mathbf{R}_b)$ is the $(k-1)$th order electric-field derivative operator, which probes the field derivative produced by subsystem A at point $\mathbf{R}_b$. $M^{(k)}_b$ and $\bar{M}^{(k)}_b$ are the $|k|$th order permanent and induced multipole moments of subsystem b, respectively. The latter is determined by equating the right-hand sides of Eqs. (52) and (53) to give

$$\forall b \in B: \quad \bar{M}^{(k)}_b = \sum_{|l|=1}^{\infty} \frac{1}{l!} P^{(k,l)}_b F^{\mathrm{tot}(l)}(\mathbf{R}_b) = \sum_{|l|=1}^{\infty} \frac{1}{l!} P^{(k,l)}_b \left(\langle \hat{F}^{(l)}_A(\mathbf{R}_b) \rangle_{0_A} + \sum_{b'\in B\setminus b} \left[\langle \hat{F}^{(l)}_{b'}(\mathbf{R}_b) \rangle^{(0)}_{0_{b'}} + \sum_{|m|=1}^{\infty} \frac{(-1)^{|m|+1}}{m!} T^{(m+l)}_{b'b} \bar{M}^{(m)}_{b'} \right] \right), \tag{54}$$

where $F^{\mathrm{tot}(l)}(\mathbf{R}_b)$ is the total $(l-1)$th order electric-field derivative acting on subsystem b. As follows from the second equality, it consists of the physical electric-field contributions from the nuclei and electrons in subsystem A and the permanent multipoles of the other environment subsystems, collectively denoted as $F^{(l)}(\mathbf{R}_b)$, as well as the contribution from the remaining first-order induced multipole moments. Hence, the first term describes the mutual coupling between subsystem A with all environment subsystems, whereas the second and third terms account for the mutual polarization between the environment subsystems.

In practice, the multipole expansions in Eqs. (51) and (52) are terminated at a finite order K_s, and to improve the convergence properties of the multipole representation, distributed multipole expansions (using $S = \sum_{b\in B} S_b$ to denote the total number of expansion points) are used instead of one-center expansions. For the expansion over induced moments in Eqs. (52) and (54), the dipole approximation is introduced and only the dipole–dipole polarizability tensor is taken into account; Eq. (54) then gives a set of coupled equations determining the induced dipole moments[57]

$$\bar{\boldsymbol{\mu}}_s(0) = \sum_{s'=1}^{S} \boldsymbol{\mathcal{R}}_{ss'}(0) \mathbf{F}(\mathbf{R}_{s'}) \,, \tag{55}$$

where the polarizability tensors for the individual sites have been replaced by a $(3S \times 3S)$-dimensional classical linear response matrix (or relay matrix) given by

$$\boldsymbol{\mathcal{R}}(\omega) = \begin{pmatrix} \boldsymbol{\alpha}_1(\omega)^{-1} & -\mathbf{T}^{(2)}_{12} & \cdots & -\mathbf{T}^{(2)}_{1S} \\ -\mathbf{T}^{(2)}_{21} & \boldsymbol{\alpha}_2(\omega)^{-1} & \ddots & \vdots \\ \vdots & \ddots & \ddots & -\mathbf{T}^{(2)}_{(S-1)S} \\ -\mathbf{T}^{(2)}_{S1} & \cdots & -\mathbf{T}^{(2)}_{S(S-1)} & \boldsymbol{\alpha}_S(\omega)^{-1} \end{pmatrix}^{-1} . \tag{56}$$

This matrix holds the inverse of the distributed electronic dipole–dipole polarizability tensors on the diagonal and second-order interaction tensors in the off-diagonal blocks. Upon contraction with unit vectors, $\boldsymbol{\mathcal{R}}(\omega)$ models the electronic dipole–dipole polarizability of the environment.[57]

By combining Eqs. (51) and (53) in truncated and distributed forms, we finally obtain the embedding operator defining the PE model,

$$\hat{v}_{\mathrm{PE}} = \sum_{pq\in A} \sum_{s=1}^{S} \sum_{|k|=0}^{K_s} \frac{(-1)^{|k|}}{k!} M^{(k)}_s t^{(k)}_{pq}(\mathbf{R}_s) \hat{E}_{pq} - \sum_{s=1}^{S} \bar{\mu}_{s,\alpha}(0) \hat{F}^{\mathrm{e}}_{A,\alpha}(\mathbf{R}_s) \,. \tag{57}$$

The induced dipoles, and in turn the embedding operator, depend on the wave function of subsystem A through the electric fields. In other words, upon averaging over the environment wave functions, the Hamiltonian turns into a nonlinear effective operator.

2. Response theory framework

Let us now proceed to the quantum-mechanical response framework within PE. This extension usually proceeds by assuming the classical description of the environment from the outset, i.e., starting from Eq. (57) and the associated energy functional [see, e.g., Eq (21) in Ref. 51]. We shall instead begin from the response expressions derived in Sec. II B and show, by taking the proper limits, how the PE response relations are

recovered. As briefly alluded to in Sec. II B 3, the differentiated treatment in the PE model is achieved by the perturbation analysis of the quantities in the linear response function although, as we will presently discuss, the choice of truncation is not fully coherent from a perturbation theory point of view. Since special attention is given to subsystem A, and the sole purpose of subsystem B in this context is to obtain a realistic description of the properties of A, the order counting will be performed on the effective subsystem A quantities.

As a first step toward the PE model, one includes terms in the pure subsystem A blocks and vectors through second order [in the meaning of Eq. (S13) in the supplementary material], using a first-order corrected wave function for the environment normalized through second order. The pure B blocks as well as the coupling blocks are evaluated only through lowest non-vanishing order. That is, only the zeroth-order contribution to the wave function of the environment subsystem is included. For the electronic Hessian, this implies that the $\mathbf{E}_B^{[2]}$ and $\mathbf{E}_{AB}^{[2]}$ matrices must be known through zeroth and first orders, respectively. Accordingly, the electronic Hessian and metric matrices are approximated as

$$\mathbf{E}^{[2]} = \begin{bmatrix} \mathbf{E}_A^{[2](0,1,2)} & \mathbf{E}_{AB}^{[2](1)} \\ \mathbf{E}_{AB}^{[2](1)} & \mathbf{E}_B^{[2](0)} \end{bmatrix}, \qquad \mathbf{S}^{[2]} = \begin{bmatrix} \mathbf{S}_A^{[2](0,1,2)} & \mathbf{0} \\ \mathbf{0} & \mathbf{S}_B^{[2](0)} \end{bmatrix}. \tag{58}$$

Although the pure B block is treated only through zeroth order, its effect on excitations in A is correct through second order as can be seen from the resulting effective electronic Hessian for subsystem A,

$$\widetilde{\mathbf{E}}_A^{[2]} \overset{\text{(II)}}{=} \underbrace{\mathbf{E}_A^{[2](0,1,2)}}_{\text{I}} - \underbrace{\mathbf{E}_{AB}^{[2](1)}(\mathbf{E}_B^{[2](0)} - \omega\mathbf{S}_B^{[2](0)})^{-1}\mathbf{E}_{BA}^{[2](1)}}_{\text{II}}. \tag{59}$$

This order truncation thus provides excitation energies of A-dominated transitions that are consistent through second order. The explicit expressions for the terms are given by

$$\text{I} = \langle 0_A | \, [\mathbf{Q}_A, [\hat{\mathcal{H}}_A + \hat{\mathcal{V}}^{\text{int}}, \mathbf{Q}_A^\dagger]] \, | 0_A \rangle, \tag{60}$$

$$\text{II} = \mathbf{V}_{\hat{\mathcal{V}}_{\mathbf{r}}^A} C_{\mathbf{r},\mathbf{r}'}^{B,(0)}(\omega) \mathbf{V}_{\hat{\mathcal{V}}_{\mathbf{r}'}^A}^\dagger, \tag{61}$$

using Eq. (48) for a single environment subsystem and implying that $|0_A\rangle$ has been derived from the effective Hamiltonian including Eq. (48) rather than the full operator in Eq. (8). The metric matrices retain their structures in Eq. (16). Based on the chosen truncation, the expression for the effective property gradient for subsystem A becomes

$$\widetilde{\mathbf{V}}_{A,\alpha}^{\omega} = \mathbf{V}_{A,\alpha}^{\omega(2)} - \mathbf{E}_{AB}^{[2](1)}(\mathbf{E}_B^{[2](0)} - \omega\mathbf{S}_B^{[2](0)})^{-1}\mathbf{V}_{B,\alpha}^{\omega(0)}. \tag{62}$$

For this reason, the analogy to SOPPA is imperfect; keeping only the zeroth-order correction to the B part of the property gradients means that the effective transition moments and thereby the linear response function are not consistent through second order.

To arrive at the PE model, we further need to decompose the environment into individual subsystems and invoke a truncated multipole representation of the interaction operator with respect to the environment subsystems. For practical feasibility but without theoretical justification, the lowest-order approximation invoked for the combined environment is also employed for all individual subsystems constituting the environment, meaning that the ground-state polarization among the environment subsystems, otherwise implied in $\mathbf{E}_B^{[2](0)}$, is neglected. Taking the simplest two-subsystem environment as an example, the structure of the PE analog of II in Eq. (61) then takes the form illustrated in Fig. 1. In particular, upon rewrite of the matrix resolvent according to Eq. (26), contraction with the property gradients, and repeated use of Eq. (34) on the resulting subsystem blocks, we recognize the series expansions of the corresponding blocks in the relay matrix [Eq. (56)]. For instance, the first block can be rewritten as

$$\mathbf{V}_{\hat{\mu}^{b_1}}^{(0)\dagger}\left((\mathbf{E}_{b_1}^{[2](0)} - \omega\mathbf{S}_{b_1}^{[2](0)})^{-1} - \mathbf{E}_{b_1b_2}^{[2](1)}(\mathbf{E}_{b_2}^{[2](0)} - \omega\mathbf{S}_{b_2}^{[2](0)})^{-1} \times \mathbf{E}_{b_2b_1}^{[2](0)}\right)^{-1}\mathbf{V}_{\hat{\mu}^{b_1}}^{(0)} = \left(\boldsymbol{\alpha}_{b_1}(\omega)^{-1} + \mathbf{T}_{b_1b_2}^{(2)}\boldsymbol{\alpha}_{b_2}(\omega)\mathbf{T}_{b_2b_1}^{(2)}\right)^{-1}. \tag{63}$$

Rewriting the second term of Eq. (62) in a similar manner using the electric dipole operator as perturbation, we finally recover the PE analogs of the effective electronic Hessian and effective property gradient

$$\begin{aligned} \widetilde{\mathbf{E}}_A^{[2]} \overset{\text{PE}}{=} & \langle 0_A | \, [\mathbf{Q}_A, [\hat{\mathcal{H}}_A + \hat{v}_{\text{PE}}, \mathbf{Q}_A^\dagger]] \, | 0_A \rangle \\ & - \sum_{s,s'=1}^{S} \langle 0_A | \, [\mathbf{Q}_A, \hat{\mathbf{F}}_A^{\text{e}}(\mathbf{R}_s)] \, | 0_A \rangle \\ & \times \boldsymbol{\mathcal{R}}_{ss'}(\omega) \langle 0_A | \, [\mathbf{Q}^\dagger, \hat{\mathbf{F}}_A^{\text{e}}(\mathbf{R}_{s'})] \, | 0_A \rangle, \end{aligned} \tag{64}$$

$$\begin{aligned} \widetilde{\mathbf{V}}_{A,\alpha}^{\omega} \overset{\text{PE}}{=} & \langle 0_A | \, [\mathbf{Q}_A, \hat{V}_{A,\alpha}^{\omega}] \, | 0_A \rangle \\ & - \sum_{s,s'=1}^{S} \langle 0_A | \, [\mathbf{Q}_A, \hat{\mathbf{F}}_A^{\text{e}}(\mathbf{R}_s)] \, | 0_A \rangle \, \boldsymbol{\mathcal{R}}_{ss'}(\omega)\mathbf{e}_\alpha, \end{aligned} \tag{65}$$

where $\mathbf{e}_\alpha$ denotes a unit vector in the Cartesian direction α. These expressions are equivalent to those defined in Table 1 of Ref. 51. The above expressions define the environmental effects included in the PE model within a linear response

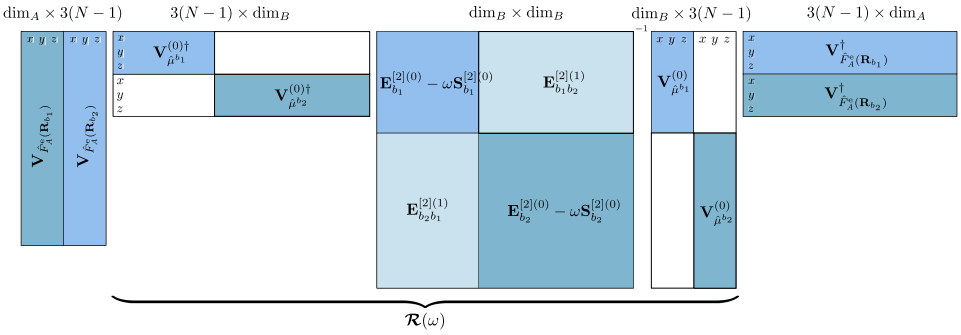

FIG. 1. Structure of the PE analog of Eq. (61) for an environment with two ($N - 1 = 2$) environment subsystems b_1 and b_2. White blocks are zero, while colored blocks represent nonzero intra- and intersubsystem blocks. Upon repeated use of Eq. (34), the expression can be written in PE terminology in terms of the relay matrix $\boldsymbol{\mathcal{R}}(\omega)$.

framework. Specifically, Eq. (64) defines the static (through $\hat{v}_{\mathrm{PE}}$) and dynamic reaction field effects (second term), while the second term of Eq. (65) defines the effective external field effect,[51] also referred to as the local field effect.[32] We remark that the effective external field effect is of the same origin as the cavity-field effect in the framework of continuum models leading to the so-called effective molecular properties[58–61] but is defined with respect to the external probing field rather than the Maxwell field within the dielectric.[51]

We have thus shown the transition from a full quantum-mechanical description of the linear response of the combined system to the differentiated subsystem treatment in the PE model. The theoretical analysis of Sec. II B can now be carried over to the present situation where only the quantum system is of interest, i.e., combining the first term of the symmetric (nonsymmetric) decomposition with the effective quantities in Eqs. (64) and (65) to obtain the subsystem A contributions to molecular (transition) properties within the PE model.

An additional and widely adopted approximation in polarizable embedding is to assume frequency-independent environment subsystems, that is, imposing $\mathbf{S}_B^{[2]} = \mathbf{0}$, which translates into taking the zero-frequency (ZF) limit of the relay matrix in Eqs. (64) and (65). In the case of optical frequencies and small spectral overlap between the quantum region and the environment, this is a good approximation because of a small frequency dispersion of the polarizabilities of the environment subsystems.[62,63] The approximation offers significant simplifications: (*i*) the nonlinearity of the effective electronic Hessian is lost such that Eq. (32) reduces to a standard generalized eigenvalue problem, (*ii*) the renormalization factor, otherwise needed in Eq. (38), becomes unity because the excitation is restricted to subsystem A in this approximation, and (*iii*) the additional zeroth-order poles in the first term of Eq. (40) are removed. Alternatively, if focus is on the spectrum and not the individual transitions, the need for an iterative solution and renormalization can also be removed by use of the complex response framework, as discussed in Sec. II B 4.

III. NUMERICAL ILLUSTRATION

To illustrate the basic features of the response of a combined system to a perturbing external field and the importance of the various intersubsystem interactions, we will in this section consider the numerical behavior of the working expressions presented in Sec. II.

A. Model system

For this purpose, we consider a simplified six-level-model (SLM) for a *para*-nitroaniline (*p*NA)–water complex and its linear response to a uniform electric-field perturbation. In addition to the respective ground states, the SLM includes also the first and second singlet excited states for *p*NA—these are the $n\pi^*$ state and the intramolecular amino-to-nitro charge-transfer transition referred to as $\pi\pi^*$—and the first and third singlet excited states for water—these are states $1B_1$ and $1A_1$, respectively, using the symmetry labels referring to the irreducible representations of the C_{2v} point group of the parent molecule. The manifold of states in the SLM is depicted in Fig. 2, defining *p*NA and water as subsystems A and B, respectively. The associated set of monomer parameters are given in Tables I and II (see computational details in Sec. S5 of the supplementary material). As expected from the strengths of the leading-order transition dipoles and their relative orientations (the charge-transfer transition is directed along the x-axis), only the electronic coupling between the $\pi\pi^*$ and $1A_1$ states is significant, whereas the $n\pi^*$ and $1B_1$ states will essentially be unaffected. However, the state mixing still remains small because their energy difference is significantly larger than their electronic coupling. Therefore, to better illustrate the different aspects of the response of a combined system, the coupling blocks of the electronic Hessian have been scaled (by an arbitrary factor of 12). The largest absolute intersubsystem coupling element is then equal to

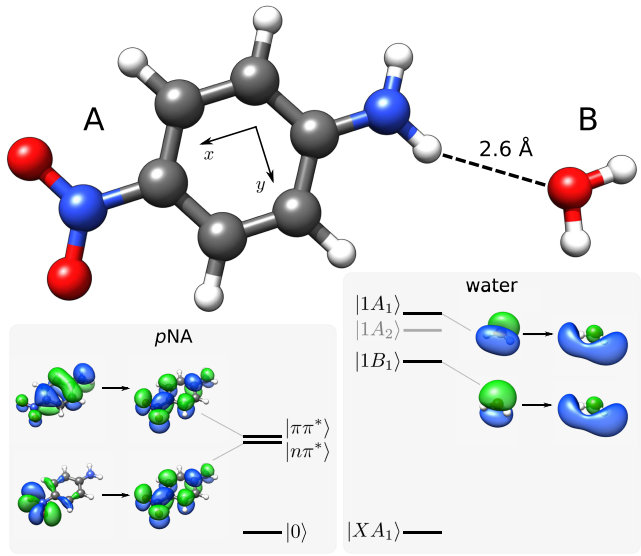

FIG. 2. The six-level-model used for the *p*NA–water complex with isosurfaces of the orbitals mainly involved in the considered transitions (shown in black).

TABLE I. The polarized subsystem parameters used in the SLM for the *p*NA–water complex in Fig. 2. All results are reported in a.u. and have been obtained at the CAM-B3LYP/aug-cc-pVDZ level of theory in the presence of the ground-state-frozen PE embedding potential of the other subsystem.

State	ΔE	$\lvert\mu_x\rvert$	$\lvert\mu_y\rvert$	$\lvert\mu_z\rvert$
$\lvert n\pi^*\rangle$	0.140 14	0.001 02	0.000 17	0.000 23
$\lvert\pi\pi^*\rangle$	0.154 28	2.022 74	0.000 30	0.005 39
$\lvert 1B_1\rangle$	0.268 14	0.073 02	0.026 34	0.540 89
$\lvert 1A_1\rangle$	0.350 27	0.425 22	0.496 12	0.091 83

TABLE II. Absolute (unscaled) electronic couplings used in the SLM for the *p*NA–water complex in Fig. 2. Digits in parentheses refer to negative exponents, i.e., $a(b) = a \times 10^{-b}$. All results are reported in a.u. and have been obtained at the CAM-B3LYP/aug-cc-pVDZ level of theory in the presence of the ground-state-frozen PE embedding potential of the other subsystem.

pNA\water	$\lvert 1B_1\rangle$	$\lvert 1A_1\rangle$
$\lvert n\pi^*\rangle$	2.53(6)	1.03(6)
$\lvert\pi\pi^*\rangle$	3.82(6)	1.76(3)

0.0212 a.u., which is smaller than the relevant difference between the excitation energies in the subsystems by a factor of ∼9.

B. Subsystem decomposition: Electric polarizability

Figure 3(a) shows the total isotropic electric dipole–dipole polarizability, as given by Eq. (12), of the *p*NA–water complex within the SLM. The excitation energies of the full system and hence the poles of the linear response are indicated by the vertical dotted lines. In the frequency region around the two lowest poles (0.10 − 0.20 a.u.), the isotropic polarizability is dominated by the α_{xx} component of the tensor with a dispersion that in turn is dictated by the $\pi\pi^*$-transition (second pole). This leads to the seemingly absence of a pole at the first excitation in subsystem A, which is a mere consequence of the $n\pi^*$-transition being nearly electric-dipole forbidden and close in energy to the intense $\pi\pi^*$-transition.

Let us now consider the symmetric decomposition of the polarizability into subsystem A and B contributions according to Eq. (27) [Fig. 3(b)]. In contrast to the total polarizability of the combined system, the diagonal elements of the individual subsystem contributions in the static limit are not guaranteed to be positive. As follows from Eq. (30), there are two contributions to the modified property gradient, e.g., $\widetilde{\mathbf{V}}^{\omega}_{A,\beta}$. The contribution from the first term, i.e., $\mathbf{V}^{\omega}_{A,\beta}$, indeed gives a positive contribution to the diagonal element of the static subsystem A response function, whereas this does not hold for the second term. When the response of subsystem B to the external field is large, the second term in the effective property gradient

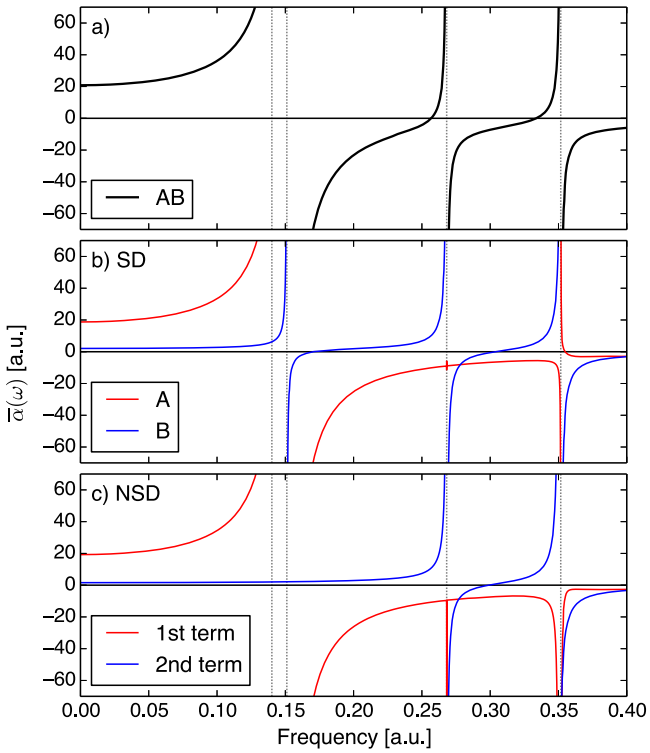

FIG. 3. Isotropic electric dipole–dipole polarizability adopting the SLM in Fig. 2. (a) For the combined system as given by Eq. (12), (b) the symmetric decomposition according to Eq. (27), and (c) the nonsymmetric decomposition according to Eq. (35). Vertical dotted lines indicate the resonance frequencies of the combined system.

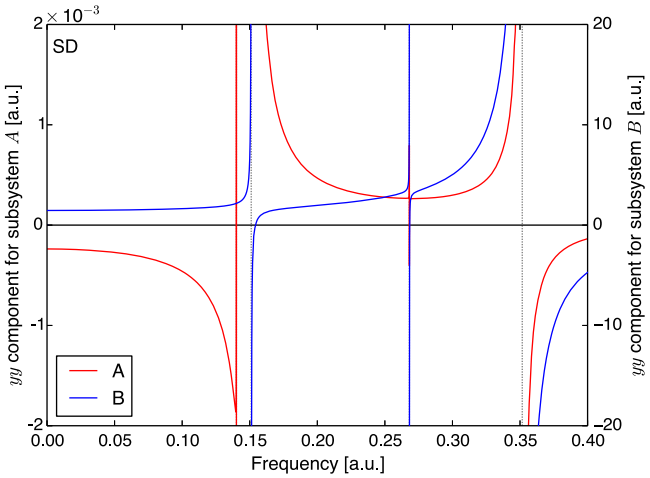

FIG. 4. Symmetric subsystem contributions to the yy component of the electric dipole–dipole polarizability of the combined system adopting the SLM in Fig. 2. Note the different scales used for the two y-axes. The vertical dotted lines indicate the resonance frequencies of the combined system.

dominates and leads to an overall negative value. This situation is exemplified by the subsystem A contribution to $\alpha_{yy}(0)$ shown in Fig. 4.

Figure 3(b) clearly shows that both the subsystem A and B contributions in the symmetric decomposition contain poles at *all* the excitation energies of the combined system, also referred to as the physical excitations. As we discussed in Sec. II B 3, this implies that transition moments, in contrast to excitation energies, cannot be determined from any single one of the terms. Turning to the nonsymmetric decomposition [Eq. (35)] shown in Fig. 3(c), on the other hand, all the physical poles are collected in the first term, and it is thus the proper choice when determining residues for the transitions mainly located in subsystem A. In addition to the physical poles, however, there are unphysical zeroth-order poles in the first term that are removed by the second term of Eq. (35) to give the total polarizability. Specifically, they contain poles at the excitation energies of subsystem B within the FP approximation, i.e., where the environment polarization is fixed during the response calculation. This inclusion of both physical and unphysical poles in the first term of Eq. (35) becomes particularly apparent in the frequency region close to the fourth excitation [red solid line in Fig. 3(c) at ∼0.35 a.u.].

C. Subsystem decomposition: Electric transition properties

The excitation energies and associated one-photon transition strengths are reported in Table III for the two lowest transitions in the model system, i.e., those predominantly localized in subsystem A. First, the results provide clear evidence for the equivalence between the properties obtained from the decomposed subsystem expressions in Eqs. (32) and (38) and from the consideration of the full system expressed in terms of Eq. (21). We further consider various approximate models that are defined according to what terms are retained in the response expressions: (*i*) The impact of the renormalization factor defined in Eq. (37) and appearing in Eq. (38) depends on the degree of delocalization of the given transition, and its neglect (denoted by "−renorm" in Table III) leads

TABLE III. Excitation energies and one-photon transition strengths for the two lowest-lying (i.e., subsystem *A*-dominated) electronic transitions in the composite system as computed from the full treatment as well as the nonsymmetric decomposition (NSD), including and excluding various contributions. All results are reported in a.u. and digits in parentheses refer to negative exponents, i.e., $a(b) = a \times 10^{-b}$. Vac: vacuum, FP: frozen ground-state environment polarization, renorm: renormalization, EEF: effective external field, ZF: zero-frequency approximation for the environment.

	$\|1_{AB}\rangle$				$\|2_{AB}\rangle$			
Model	ΔE	$\|\mu_x\|^2$	$\|\mu_y\|^2$	$\|\mu_z\|^2$	ΔE	$\|\mu_x\|^2$	$\|\mu_y\|^2$	$\|\mu_z\|^2$
Vac	0.139 50	6.0205(7)	3.3384(8)	6.6642(9)	0.156 25	4.0014	6.5832(7)	4.3947(5)
FP	0.140 14	1.4022(6)	3.0284(8)	5.1435(8)	0.154 28	4.0915	8.8700(8)	2.9025(5)
Full system		1.9202(6)	4.8179(8)	2.2571(9)		4.3996	5.4416(3)	3.5539(4)
NSD [Eq. (38)]		1.9202(6)	4.8179(8)	2.2571(9)		4.3996	5.4416(3)	3.5539(4)
NSD(−renorm)	0.140 14	1.9202(6)	4.8179(8)	2.2571(9)	0.151 10	4.4423	5.4944(3)	3.5884(4)
NSD(−EEF)		1.8561(6)	3.0263(8)	5.1047(8)		4.1373	8.9645(8)	2.9350(5)
NSD(−(renorm/EEF))		1.8561(6)	3.0263(8)	5.1047(8)		4.1774	9.0515(8)	2.9635(5)
NSD(+ZF)	0.140 14	1.7309(6)	4.4586(8)	9.1521(9)	0.151 70	4.3745	3.6180(3)	2.7005(4)

to an overestimation of transition strengths, as expected. (*ii*) The effective field strengths experienced by subsystem *A* in the presence of subsystem *B* [Eq. (30)] can be different for different directions as a consequence of the anisotropy of the polarizability of *B* and the relative orientation of the interacting subsystems. This is seen by comparing to the assumption that only subsystem *A* interacts with the external field (denoted by "−EEF" in Table III). In other words, the influence of the EEF is not just a simple scaling as opposed to the renormalization. Furthermore, as seen from the present example, the impact of renormalization is smaller than that of the EEF effect for excitations in subsystem *A* far from resonances in *B* (the environment). This is expected from the relative dependency on the energy denominator of the two contributions.

D. Frequency-independent effective subsystem Hessian

As discussed in Sec. II C 2, various polarizable embedding models typically assume the effective electronic Hessian of subsystem *A* to be frequency-independent, thereby losing the nonlinearity of the linear response equations and the poles associated with excitations predominantly in subsystem *B*. The impact of the ZF limit on the poles is illustrated in Fig. 5 by the inverse of the isotropic polarizability of the combined system. Associated excitation energies and transition moments are given in Table III. As anticipated from the weak dispersion of the real polarizability for subsystem *B* at the resonance frequencies in subsystem *A* [see Fig. 3(c)], the neglect of transitions in subsystem *B* only leads to small changes in the transition properties of the *A*-dominated excitations. We also remark that the ZF approximation is analogous to the familiar adiabatic approximation in time-dependent DFT (TD-DFT) where the exchange correlation kernel is assumed to be frequency-independent and hence leads to a linear eigenvalue problem with solutions only at Kohn–Sham one-electron excitations.[64–66] Double- and higher-electron excitations and their effects on the Kohn–Sham single excitations are thus neglected in adiabatic TD-DFT,[67] as are the excitations in subsystem *B* in our case.

E. Intensity borrowing

Let us now consider the effect of subsystem *B* on transition strengths of *A*-dominated excitations. As discussed in Sec. II B 4, the coupling of subsystem excitations gives rise to intensity borrowing. To illustrate this effect, we report in Fig. 6(a) the linear absorption cross section defined in Eq. (43) for the full system together with that associated with subsystem *A*, i.e., the first term of Eq. (40). In Fig. 6(b), the corresponding cross sections for the subsystems within the FP approximation are reported. Upon integrating the absorption cross section for the full system [black solid line in Fig. 6(a)] across the full frequency range, we obtain a reference value of $I_{AB} = 0.0829$ a.u. Due to the very limited description of the electronic structure of the *p*NA–water complex by means of the SLM, this value is far from the exact value of 11.81 a.u. as obtained from the conservation law in Eq. (44) for a system with 82 electrons. This discrepancy is of no concern here since the key point is that the value for the integrated cross section is identical to the corresponding summed result for the two subsystems within

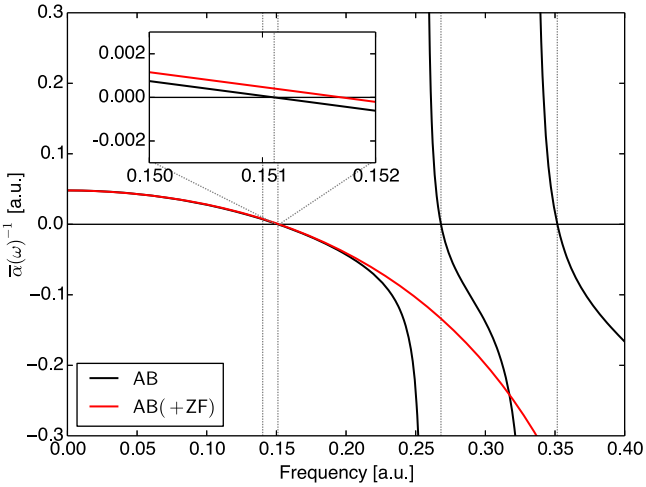

FIG. 5. Frequency-dependency of the inverse of the isotropic electric dipole–dipole polarizability of the *p*NA–water complex within the SLM when including the dynamic response of water compared to the ZF limit. This approximation reduces the number of poles to the number of excitations in subsystem *A* and blue-shifts the excitation energies (see inset).

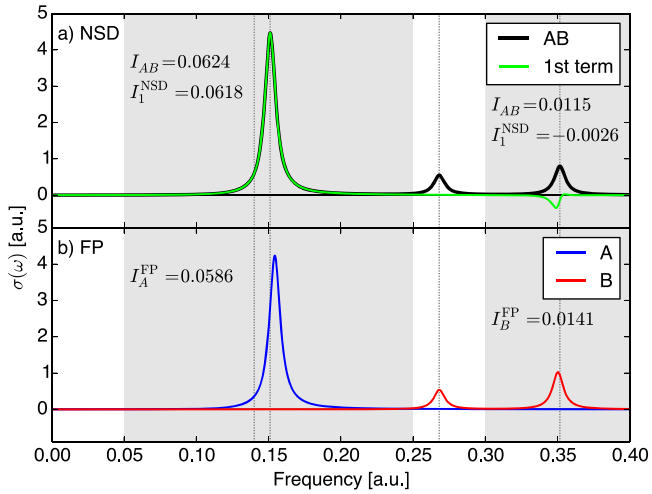

FIG. 6. The linear absorption cross section for *p*NA–water complex within the SLM. (a) Integrated absorption cross sections (in a.u.) are reported for the intervals indicated by the gray-shaded areas. A common damping parameter of 4.5566×10^{-3} a.u. was used for all transitions. The vertical dotted lines indicate the resonance frequencies of the combined system.

the FP approximation ($I_A^{\rm FP} = 0.0606$ and $I_B^{\rm FP} = 0.0223$ a.u., respectively). Let us now pass to examine the nonsymmetric decomposition in Eq. (40) with individual cross sections $\sigma_1^{\rm NSD}(\omega)$ and $\sigma_2^{\rm NSD}(\omega)$ obeying their own respective conservation laws as expressed in Eq. (47). Since the nonsymmetric decomposition is made such that the second term corresponds exactly to subsystem B within the FP approximation, the cross section $\sigma_2^{\rm NSD}(\omega)$ is identical to the red solid line in Fig. 6(b).

Finally, we include in Fig. 6 also the partially integrated absorption cross section for two separate finite energy intervals, shown as gray-shaded areas in the figure. In agreement with the increase in transition strength found in Table III, the lowest band dominated by the $\pi\pi^*$ state is intensified upon coupling the excitations in the two subsystems. This intensity gain in one part of the spectrum is counteracted by a reduction of the intensity in another part, and in the nonsymmetric decomposition, this will be seen only in $\sigma_1^{\rm NSD}(\omega)$. Since the coupling of the lowest subsystem A-dominated band (second transition) is only effective to the subsystem B-dominated $1A_1$-band (fourth transition), there will be an intensity borrowing from the latter to the former. As a consequence, $\sigma_1^{\rm NSD}(\omega)$ will take on negative values in the region of the fourth transition (∼0.35 a.u.) as seen in Fig. 6(a) (green solid line). Accordingly, in frequency regions dominated by transitions in subsystem A, the calculation of $\sigma_1^{\rm NSD}(\omega)$ is to be associated with an absorption spectrum, whereas this cannot be readily done in frequency regions that includes transitions in subsystem B.

IV. SUMMARY AND CONCLUSIONS

In this work, we have provided a rigorous derivation of the various terms appearing in linear response theory of a quantum molecular system embedded in a polarizable environment. The origin of the three distinct mechanisms for environmental effects within polarizable embedding in a linear response framework—the static and dynamic environment responses as well as the effective external field effect—follows straightforwardly from a subsystem decomposition of a quantum-mechanical direct-product treatment of the response of the entire system.

A crucial point is what decomposed form of the response function that ought to be used in a given context. Our theoretical analysis and numerical inspection of the basic features of two alternative subsystem decompositions have clarified such discussions and highlighted some potential issues in defining subsystem contributions to response and transition properties.

Our first, symmetric decomposition given in Eq. (27) treats subsystems on an equal footing and results in two linear response function terms that express the permutation of subsystem indices. This is the natural choice for computing subsystem contributions to molecular properties, but, as also shown in the framework of subsystem DFT,[48] the coupling of the subsystems manifests itself in that each subsystem contribution contains the poles of the entire system. As a result that is made clear in the present work, transition strengths for a subsystem-dominated excitation cannot be found from the residue analysis of the symmetric subsystem linear response function.

Our second, nonsymmetric decomposition given in Eq. (35) treats, on the other hand, subsystems on an unequal footing and results in two linear response function terms that both are symmetric with respect to left and right property gradients. This is an unnatural choice for the development of polarizable embedding models due to the fact that the (first) term of dimension of the excitation manifold of the quantum region contains poles not only from all transitions in the fully interacting system but also poles from the ground-state polarized, but otherwise uncoupled, environment. We demonstrated that the nonsymmetric decomposition lends itself to the determination of transition strengths but only after taking proper account of renormalization of the subsystem excitation vectors. The renormalization factor is however not accessible within the framework of polarizable embedding. This complication can be avoided in practice by assuming the static limit for the environment response or by turning to the framework of complex linear response theory. We have shown that the integrated absorption cross sections of the two terms in the nonsymmetric decomposition are preserved independently of each another, and as a consequence, the subsystem absorption cross sections (and likewise oscillator strengths) will take on negative values if intersubsystem intensity borrowing takes place.

SUPPLEMENTARY MATERIAL

See supplementary material for computational details and derivations of Eqs. (31), (44), and (51)–(53).

ACKNOWLEDGMENTS

N.H.L. thanks J. Oddershede (University of Southern Denmark, Odense, Denmark) for helpful discussions and the Carlsberg Foundation for a postdoctoral fellowship (Grant

No. CF15-0792). P.N. acknowledges financial support from the Swedish Research Council (Grant No. 621-2014-4646). J.K. thanks the Danish Council for Independent Research (the Sapere Aude program) and the Villum Foundation for financial support. Computation/simulation for the work described in this paper has been supported by the DeIC National HPC Center, University of Southern Denmark (SDU).

[1]M. S. Gordon, D. G. Fedorov, S. R. Pruitt, and L. V. Slipchenko, "Fragmentation methods: A route to accurate calculations on large systems," Chem. Rev. **112**, 632–672 (2012).
[2]C. R. Jacob and J. Neugebauer, "Subsystem density-functional theory," Wiley Interdiscip. Rev.: Comput. Mol. Sci. **4**, 325–362 (2014).
[3]A. S. P. Gomes and C. R. Jacob, "Quantum-chemical embedding methods for treating local electronic excitations in complex chemical systems," Annu. Rep. Prog. Chem., Sect. C: Phys. Chem. **108**, 222–277 (2012).
[4]T. A. Wesolowski and A. Warshel, "Frozen density functional approach for *ab initio* calculations of solvated molecules," J. Phys. Chem. **97**, 8050–8053 (1993).
[5]T. A. Wesolowski and J. Weber, "Kohn-Sham equations with constrained electron density: An iterative evaluation of the ground-state electron density of interacting molecules," Chem. Phys. Lett. **248**, 71–76 (1996).
[6]P. Cortona, "Self-consistently determined properties of solids without band-structure calculations," Phys. Rev. B **44**, 8454 (1991).
[7]T. A. Wesolowski, S. Shedge, and X. Zhou, "Frozen-density embedding strategy for multilevel simulations of electronic structure," Chem. Rev. **115**, 5891–5928 (2015).
[8]A. Warshel and M. Levitt, "Theoretical studies of enzymatic Reactions: Dielectric, electrostatic and steric stabilization of the carbonium ion in the reaction of lysozyme," J. Mol. Biol. **103**, 227–249 (1976).
[9]H. M. Senn and W. Thiel, "QM/MM methods for biomolecular systems," Angew. Chem., Int. Ed. **48**, 1198–1229 (2009).
[10]M. W. van der Kamp and A. J. Mulholland, "Combined quantum mechanics/molecular mechanics (QM/MM) methods in computational enzymology," Biochemistry **52**, 2708–2728 (2013).
[11]P. E. M. Lopes, B. Roux, and A. D. MacKerell, Jr., "Molecular modeling and dynamics studies with explicit inclusion of electronic polarizability: Theory and applications," Theor. Chem. Acc. **124**, 11–28 (2009).
[12]M. E. Casida and T. A. Wesołowski, "Generalization of the Kohn–Sham equations with constrained electron density formalism and its time-dependent response theory formulation," Int. J. Quantum Chem. **96**, 577–588 (2004).
[13]S. Höfener, A. S. P. Gomes, and L. Visscher, "Molecular properties via a subsystem density functional theory formulation: A common framework for electronic embedding," J. Chem. Phys. **136**, 044104 (2012).
[14]J. Neugebauer, "Chromophore-specific theoretical Spectroscopy: From subsystem density functional theory to mode-specific vibrational spectroscopy," Phys. Rep. **489**, 1–87 (2010).
[15]J. Neugebauer, "On the calculation of general response properties in subsystem density functional theory," J. Chem. Phys. **131**, 084104 (2009).
[16]J. Neugebauer, "Couplings between electronic transitions in a subsystem formulation of time-dependent density functional theory," J. Chem. Phys. **126**, 134116 (2007).
[17]J. M. H. Olsen, K. Aidas, and J. Kongsted, "Excited states in solution through polarizable embedding," J. Chem. Theory Comput. **6**, 3721–3734 (2010).
[18]F. Lipparini, C. Cappelli, and V. Barone, "Linear response theory and electronic transition energies for a fully polarizable QM/classical Hamiltonian," J. Chem. Theory Comput. **8**, 4153–4165 (2012).
[19]S. Yoo, F. Zahariev, A. Sok, and M. S. Gordon, "Solvent effects on optical properties of molecules: A combined time-dependent density functional theory/effective fragment potential approach," J. Chem. Phys. **129**, 144112 (2008).
[20]L. Jensen, P. T. van Duijnen, and J. G. Snijders, "A discrete solvent reaction field model for calculating molecular linear response properties in solution," J. Chem. Phys. **119**, 3800–3809 (2003).
[21]S. M. Morton and L. Jensen, "A discrete interaction model/quantum mechanical method to describe the interaction of metal nanoparticles and molecular absorption," J. Chem. Phys. **135**, 134103 (2011).
[22]C. Curutchet, A. Muñoz-Losa, S. Monti, J. Kongsted, G. D. Scholes, and B. Mennucci, "Electronic energy transfer in condensed phase studied by a polarizable QM/MM model," J. Chem. Theory Comput. **5**, 1838–1848 (2009).
[23]C. R. Jacob, J. Neugebauer, L. Jensen, and L. Visscher, "Comparison of frozen-density embedding and discrete reaction field solvent models for molecular properties," Phys. Chem. Chem. Phys. **8**, 2349–2359 (2006).
[24]J. L. Payton, S. M. Morton, J. E. Moore, and L. Jensen, "A discrete interaction model/quantum mechanical method for simulating surface-enhanced Raman spectroscopy," J. Chem. Phys. **136**, 214103 (2012).
[25]M. N. Pedersen, E. D. Hedegrd, J. M. H. Olsen, J. Kauczor, P. Norman, and J. Kongsted, "Damped response theory in combination with polarizable environments: The polarizable embedding complex polarization propagator method," J. Chem. Theory Comput. **10**, 1164–1171 (2014).
[26]N. H. List, H. J. Aa. Jensen, J. Kongsted, and E. D. Hedegård, "A unified framework for the polarizable embedding and continuum methods within multiconfigurational self-consistent field theory," Adv. Quantum Chem. **66**, 195 (2013).
[27]J. M. H. Olsen and J. Kongsted, "Molecular properties through polarizable embedding," Adv. Quantum Chem. **61**, 107–143 (2011).
[28]N. H. List, J. M. H. Olsen, and J. Kongsted, "Excited states in large molecular systems through polarizable embedding," Phys. Chem. Chem. Phys. **18**, 20234–20250 (2016).
[29]J. M. H. Olsen, C. Steinmann, K. Ruud, and J. Kongsted, "Polarizable density embedding: A new QM/QM/MM-based computational strategy," J. Phys. Chem. A **119**, 5344–5355 (2015).
[30]T. Schwabe, "General theory for environmental effects on (vertical) electronic excitation energies," J. Chem. Phys. **145**, 154105 (2016).
[31]S. Corni, R. Cammi, B. Mennucci, and J. Tomasi, "Electronic excitation energies of molecules in solution within continuum solvation models: Investigating the discrepancy between state-specific and linear-response methods," J. Chem. Phys. **123**, 134512 (2005).
[32]L. Jensen, M. Swart, and P. T. van Duijnen, "Microscopic and macroscopic polarization within a combined quantum mechanics and molecular mechanics model," J. Chem. Phys. **122**, 034103 (2005).
[33]R. McWeeny and B. T. Sutcliffe, *Methods of Molecular Quantum Mechanics*, 2nd ed. (Academic press, London, 1989), Vol. 2.
[34]A. Stone, *The Theory of Intermolecular Forces* (Oxford University Press, 2002).
[35]T. Helgaker, P. Jørgensen, and J. Olsen, *Molecular Electronic-Structure Theory* (Wiley, 2000).
[36]J. G. Ángyán, "Common theoretical framework for quantum chemical solvent effect theories," J. Math. Chem. **10**, 93–137 (1992).
[37]O. Christiansen, P. Jørgensen, and C. Hättig, "Response functions from Fourier component variational perturbation theory applied to a time-averaged quasienergy," Int. J. Quantum Chem. **68**, 1–52 (1998).
[38]K. Sasagane, F. Aiga, and R. Itoh, "Higher–order response theory based on the quasienergy derivatives: The derivation of the frequency–dependent polarizabilities and hyperpolarizabilities," J. Chem. Phys. **99**, 3738–3778 (1993).
[39]J. Olsen and P. Jørgensen, "Linear and nonlinear response functions for an exact state and for an MCSCF state," J. Chem. Phys. **82**, 3235–3264 (1985).
[40]J. Olsen and P. Jørgensen, in *Modern Electronic Structure Theory*, edited by D. R. Yarkony (World Scientific, 1995), Vol. 2, pp. 857–990.
[41]R. Cammi, S. Corni, B. Mennucci, and J. Tomasi, "Electronic excitation energies of molecules in solution: State specific and linear response methods for nonequilibrium continuum solvation models," J. Chem. Phys. **122**, 104513 (2005).
[42]N. H. List, "Theoretical description of electronic transitions in large molecular systems in the optical and x-ray regions," Ph.D. thesis, University of Southern Denmark, Odense, Denmark, 2015.
[43]N. H. List, S. Coriani, O. Christiansen, and J. Kongsted, "Identifying the Hamiltonian structure in linear response theory," J. Chem. Phys. **140**, 224103 (2014).
[44]P.-O. Löwdin, "Studies in perturbation theory. V. Some aspects on the exact self-consistent field theory," J. Math. Phys. **3**, 1171–1184 (1962).
[45]P.-O. Löwdin, "Studies in perturbation theory: Part I. An elementary iteration-variation procedure for solving the Schrödinger equation by partitioning technique," J. Mol. Spectrosc. **10**, 12–33 (1963).
[46]P.-O. Löwdin, "Studies in perturbation theory. IV. Solution of eigenvalue problem by projection operator formalism," J. Math. Phys. **3**, 969–982 (1962).

[47]C.-P. Hsu, G. R. Fleming, M. Head-Gordon, and T. Head-Gordon, "Excitation energy transfer in condensed media," J. Chem. Phys. **114**, 3065–3072 (2001).
[48]M. Pavanello, "On the subsystem formulation of linear-response time-dependent DFT," J. Chem. Phys. **138**, 204118 (2013).
[49]E. S. Nielsen, P. Jørgensen, and J. Oddershede, "Transition moments and dynamic polarizabilities in a second order polarization propagator approach," J. Chem. Phys. **73**, 6238–6246 (1980).
[50]A. Dreuw and M. Wormit, "The algebraic diagrammatic construction scheme for the polarization propagator for the calculation of excited states," Wiley Interdiscip. Rev.: Comput. Mol. Sci. **5**, 82–95 (2015).
[51]N. H. List, H. J. Aa. Jensen, and J. Kongsted, "Local electric fields and molecular properties in heterogeneous environments through polarizable embedding," Phys. Chem. Chem. Phys. **18**, 10070–10080 (2016).
[52]P. Norman, "A perspective on nonresonant and resonant electronic response theory for time-dependent molecular properties," Phys. Chem. Chem. Phys. **13**, 20519–20535 (2011).
[53]P. Norman, D. M. Bishop, H. J. Aa. Jensen, and J. Oddershede, "Nonlinear response theory with relaxation: The first-order hyperpolarizability," J. Chem. Phys. **123**, 194103 (2005).
[54]P. Norman, D. M. Bishop, H. J. Aa. Jensen, and J. Oddershede, "Near-resonant absorption in the time-dependent self-consistent field and multiconfigurational self-consistent field approximations," J. Chem. Phys. **115**, 10323–10334 (2001).
[55]R. W. Boyd, *Nonlinear Optics* (Academic Press, 2003).
[56]N. H. List, J. Kauczor, T. Saue, H. J. Aa. Jensen, and P. Norman, "Beyond the electric-dipole approximation: A formulation and implementation of molecular response theory for the description of absorption of electromagnetic field radiation," J. Chem. Phys. **142**, 244111 (2015).
[57]J. Applequist, J. R. Carl, and K.-K. Fung, "Atom dipole interaction model for molecular polarizability. Application to polyatomic molecules and determination of atom polarizabilities," J. Am. Chem. Soc. **94**, 2952–2960 (1972).
[58]C. J. F. Böttcher and P. Bordewijk, *Theory of Electric Polarization: Dielectrics in Static Fields, Vol. 1* (Elsevier Amsterdam, 1973).
[59]R. Wortmann and D. M. Bishop, "Effective polarizabilities and local field corrections for nonlinear optical experiments in condensed media," J. Chem. Phys. **108**, 1001–1007 (1998).
[60]R. Cammi, B. Mennucci, and J. Tomasi, "On the calculation of local field factors for microscopic static hyperpolarizabilities of molecules in solution with the aid of quantum-mechanical methods," J. Phys. Chem. A **102**, 870–875 (1998).
[61]S. Pipolo, S. Corni, and R. Cammi, "The cavity electromagnetic field within the polarizable continuum model of solvation," J. Chem. Phys. **140**, 164114 (2014).
[62]I. Harczuk, O. Vahtras, and H. Ågren, "Frequency-dependent force fields for QMMM calculations," Phys. Chem. Chem. Phys. **17**, 7800–7812 (2015).
[63]M. S. Nørby, O. Vahtras, P. Norman, and J. Kongsted, "Assessing frequency-dependent site polarisabilities in linear response polarisable embedding," Mol. Phys. **115**, 39 (2017).
[64]N. T. Maitra, F. Zhang, R. J. Cave, and K. Burke, "Double excitations within time-dependent density functional theory linear response," J. Chem. Phys. **120**, 5932–5937 (2004).
[65]R. J. Cave, F. Zhang, N. T. Maitra, and K. Burke, "A dressed TDDFT treatment of the 2^1A_g states of butadiene and hexatriene," Chem. Phys. Lett. **389**, 39–42 (2004).
[66]M. E. Casida and M. Huix-Rotllant, "Many-body perturbation theory (MBPT) and time-dependent density-functional theory (TD-DFT): MBPT insights about what is missing in, and corrections to, the TD-DFT adiabatic approximation," in *Density-Functional Methods for Excited States* (Springer, 2015), pp. 1–60.
[67]M. Caballero, I. d. P. Moreira, and J. M. Bofill, "A comparison model between density functional and wave function theories by means of the Löwdin partitioning technique," J. Chem. Phys. **138**, 174107 (2013).